



ADDIS ABABA UNIVERSITY
COLLEGE OF NATURAL SCIENCE
SCHOOL OF EARTH SCIENCES

**GEOLOGY, MINERAL PARAGENESIS, AND SEQUENCE STUDY OF BIKILAL
IRON MINERALIZATION IN WEST WOLLEGA; WESTERN ETHIOPIA:
IMPLICATION TO GENESIS.**



A THESIS SUBMITTED TO THE SCHOOL OF EARTH SCIENCES
ADDIS ABABA UNIVERSITY IN PARTIAL FULFILMENT OF THE REQUIREMENTS
FOR THE DEGREE OF MASTERS OF SCIENCE IN MINERAL EXPLORATION

BY: SOLOMON REBSO

DEC. 2013

ADVISORS: 1. PROF. SOLOMON TADESSE

ABBIS

ABABA

2. DR. ASFAWOSSEN ASRAT

ABBIS

ABABA

Addis Ababa
University
(Since 1950)



GEOLOGY, MINERAL PARAGENESIS, AND SEQUENCE STUDY OF BIKILAL IRON MINERALIZATION IN WEST WOLLEGA; WESTERN ETHIOPIA: IMPLICATION TO GENESIS.

A THESIS SUBMITTED TO THE SCHOOL OF EARTH SCIENCES ADDIS ABABA UNIVERSITY IN PARTIAL FULFILMENT OF THE REQUIREMENTS FOR THE DEGREE OF MASTERS OF SCIENCE IN MINERAL EXPLORATION

BY: SOLOMON REBSO

ADVISORS: 1. PROF. SOLOMON TADESSE

2. DR. ASFAWOSSEN ASRAT

DEC. 2013

**ADDIS ABABA UNIVERSITY
COLLEGE OF NATURAL SCIENCE
SCHOOL OF EARTH SCIENCES**

**GEOLOGY, MINERAL PARAGENESIS, AND SEQUENCE STUDY OF BIKILAL
IRON MINERALIZATION IN WEST WOLLEGA; WESTERN ETHIOPIA:
IMPLICATION TO GENESIS.**

BY SOLOMON REBSO

SCHOOL OF EARTH SCIENCES

APPROVED BY THE EXAMINING BOARD

Dr. SEYFU KEBEDE -----

Chairman, Department

Graduate committee

PROF. SOLOMON TADESSE -----

Advisor

Dr. ASFAWOSSEN ASRAT

Advisor

Dr. WORASH GETANEH

Examiner

Dr. MULUGETA ALENEH

Examiner

TABLE OF CONTENTS

Acknowledgment	ix
Abstract.....	xi
CHAPTER ONE - General	1
1.1. Iron Resources Potential of Ethiopia.....	4
CHAPTER TWO - Introduction	7
2.1. Location and Accessibility	7
2.2. Physiography	9
2.3. Climate, Vegetation and Population.....	10
2.4. Review of Previous Geological Works	10
2.5. Objective	15
2.5.1. General Objective	15
2.5.2. Specific Objectives	15
2.6. Methodology	16
2.6.1. Secondary Data Collection and Interpretation.....	16
2.6.2. Field Work	16
2.6.3. Petrography	17
CHAPTER THREE - Regional Geology.....	18
3.1. East African Orogony.....	18
CHAPTER FOUR - Geology of Bikilal Area.....	25
4.1. Porphyritic Olivine Gabbro.....	27
4.2. Aphanitic Olivine Gabbro	27
4.3. Hornblende Gabbro.....	28
4.4. Hornblendite Gabbro.....	30
4.5. Granite and Pegmatite Dikes.....	31
4.6. Anorthosite Gabbro	32
4.7. Field and Petrographic Results.....	37
4.8. Geological Structures	42
4.9. Drillhole Data Logging in Bikilal Intrusive Body	42

4.9.1. Drillhole Log Correlation	43
CHAPTER FIVE - Result and Discussion	46
5.1. Mineralization	46
5.2. Ore Minerals.....	49
5.3. Description of Ore Minerals.....	52
5.3.1. Magnetite	52
5.3.2. Ilmenite	54
5.3.3. Hematite.....	56
5.3.4. Goethite and Hydro- Goethite.....	56
5.3.5. Pyrrhotite.....	57
5.3.6. Chalcopyrite.....	57
5.3.7. Pyrite.....	57
5.3.8. Pentlandite.....	58
5.3.9. Gold.....	59
5.3.10. Apatite.....	60
5.4. Alteration.....	60
5.5. Paragenesis	61
5.7. Possible Hypothesis for Bikilal Iron Ore Genesis According to Different Authors	64
CHAPTER SIX - Conclusion and Recommendations.....	67
6.1. Conclusion.....	67
6.2. Recommendations	69
References.....	70
Appendix I	74
Appendix II.....	75

LIST OF FIGURES

Figure.1. World Major Producers of Iron Ore Distribution Map	2
--	---

Figure.2. Iron ore price	3
Figure.3. Location Map of Iron Occurrences and Deposits of Ethiopia taken from Geological Survey of Ethiopia, June 2010).....	6
Figure.4. Location Map of the Study Area	8
Figure.5.The suggested evolution of the Arablan-Nublan Shield	18
Figure.6. Map of the Arabian–Nubian Shield.....	19
Figure.7. Simplified geological map of the Precambrian of Western Ethiopia.....	24
Figure.8. Geological map and cross section of Bikilal intrusive gabbro	26
Figure 10. Field photo of hornblende gabbro	29
Figure.14. Photomicrographs of gabbro.	34
Figure.15. Photomicrographs	35
Figure.16. Photomicrographs.....	36
Figure.17 (A) Correlation of different borehole loges	44
Figure.17 (B) Correlation of different borehole loges	45
Figure.18. Map showing iron ore distribution in Bikilal iron ore deposit.	48
Figure. 19. Photomicrographs of magnetite, pyrite and oxidation textures of ilmenite.	53
Figure.20. Photomicrographs of oxidation textures of magnetite and ilmenite.....	55
Figure.21. Photomicrographs association of magnetite, pyrite, chalcopyrite.....	56
Figure.22. Photomicrographs showing magnetite (MAG), Pyrite (PY) & Pyrrhotite	58
Figure.23. Photomicrographs showing Gold (AU) grains	59
Figure.24. Mineral paragenetic sequences mineralization of Bikilal iron ore deposit. ..	62
Figure.25. Major Element MgO variation diagrams.....	65

LIST OF TABLES

Table.1. Field and petrographic description of different rock samples such as: olivine gabbro, hornblende gabbro, hornblendite gabbro, and anorthosite gabbro. 41

Table.2. Ore microscopic result 51

DECLARATION

I hereby declare that the work which is being presented in this thesis entitled “Geology, Mineral Paragenesis, and Sequence study of Bikilal Iron Mineralization in West Wollega; Western Ethiopia: Implication to Genesis” is original work of my own, has not been presented for a degree or diploma in any other university and that all source of the material used for the thesis have been duly acknowledged.

Solomon Rebso
(Candidate)

Date

This is to certify that the above declaration made by the candidate is correct to the best of my knowledge.

Professor Solomon Tadesse
(1st Advisor)

Date

Dr. Asfawossen Asrat
(2nd Advisor)

Date

ACKNOWLEDGMENT

First of all, I would like to thank the almighty God for the many blessings.

I have no words to thank my advisor Prof. Solomon Tadesse for his decisive guidance throughout this thesis work. The constructive suggestions and his material support he gave me were important to accomplish the work and this final manuscript. Moreover, I would like to thank him for his support in suggesting and providing valuable reference materials and sharing his field and research experiences.

I am very grateful to my second advisor Dr. Asfawossen Asrat for his persistent supervision, reviewing the thesis and providing useful comments and encouragements I received.

I also acknowledge Addis Ababa University School of Earth Sciences for the finance and equipment support that was essential for this research work accomplishment.

I want to acknowledge W/ro Workelul G/Kirstos and her co-workers from Ethiopian Geological Survey central laboratory for their exciting help during polished and thin section preparation.

I am also thankful to W/ro Tenaye Hailu senior information expert at Geological Survey of Ethiopia library for providing available secondary data and important reference materials.

I am highly indebted to Western Wollega Ghimbi Zone Water, Mining and Energy Bureau for their generous help in arranging transport facility during the field work and other logistic support.

Finally yet importantly, my sincere thank goes to my friends and my family for their unreserved encouragement patience, and help which was so vital to accomplish this work.

ABSTRACT

Bikilal iron ore deposit is a Kiruna-type magnetite – ilmenite deposit in West Wollega Western Ethiopia. It is formed within syn-post tectonic intrusive gabbroic complex that intrudes the Precambrian gneiss. Bikilal gabbroic intrusion comprises olivine gabbro in the center, hornblende gabbro and hornblendite as dominant rock at the periphery of the intrusive as well as pegmatite, granite, migmatite, and anorthosite found as a minor lithology. Generally all lithological units are dipping SW with dip angles ranging from 35° – 75° . The major structural trends in the study area are NW – SE following the regional lineament. Drill hole data shows that the rocks have layering. Hornblende gabbro and hornblendites with anorthosite are characterized by magnetite- ilmenite and apatite mineralization. Identification of different minerals and their textural relationships have been studied using ore and transmitted light microscope at the School of Earth Sciences, Addis Ababa University.

The iron ore bearing hornblendite is classified into upper zone in the northern, middle zone in the north- eastern, and lower zone in the southern part of the study area. Bikilal iron deposit consists of magnetite, ilmenite, hematite, sulphides, apatite and gold. The principal ore minerals are magnetite and ilmenite. Apatite is the second most abundant mineral in association with magnetite and ilmenite. The sulfide minerals present are pyrite, chalcopyrite, pyrrhotite and pentlandite. Gold grains are found as isolated free grain in association with other sulphide minerals but commonly it is found as hatched inclusion inside chalcopyrite.

The paragenetic sequence of mineralization was classified into four phases based on the microscopic study and existing geochemical data from previous works: **Phase I** = Silicates (olivine + pyroxene+ feldspar); **Phase II** =magnetite + massive- veinlet ilmenite + pyrite + pentlandite+ free gold; **Phase III** =exsolved ilmenite + hematite + pyrrhotite + gold; and **Phase IV**=chalcopyrite + geothite. In this work mineral association and paragenesis of Fe-Ti oxide-Py-Cu-Pyr-Ni-Au were identified and studied.

CHAPTER ONE

GENERAL

Iron is the fourth most abundant element in the earth's crust after oxygen, silicon and aluminum and is an essential commodity for modern industry (Conliffe et al., 2012). Iron is also the most abundant element by mass, making up 35% of the mass of the earth as a whole. The concentration of iron in the various layers of the earth ranges from very high at the inner core to only a few percent in the outer crust (Wood, 2011).

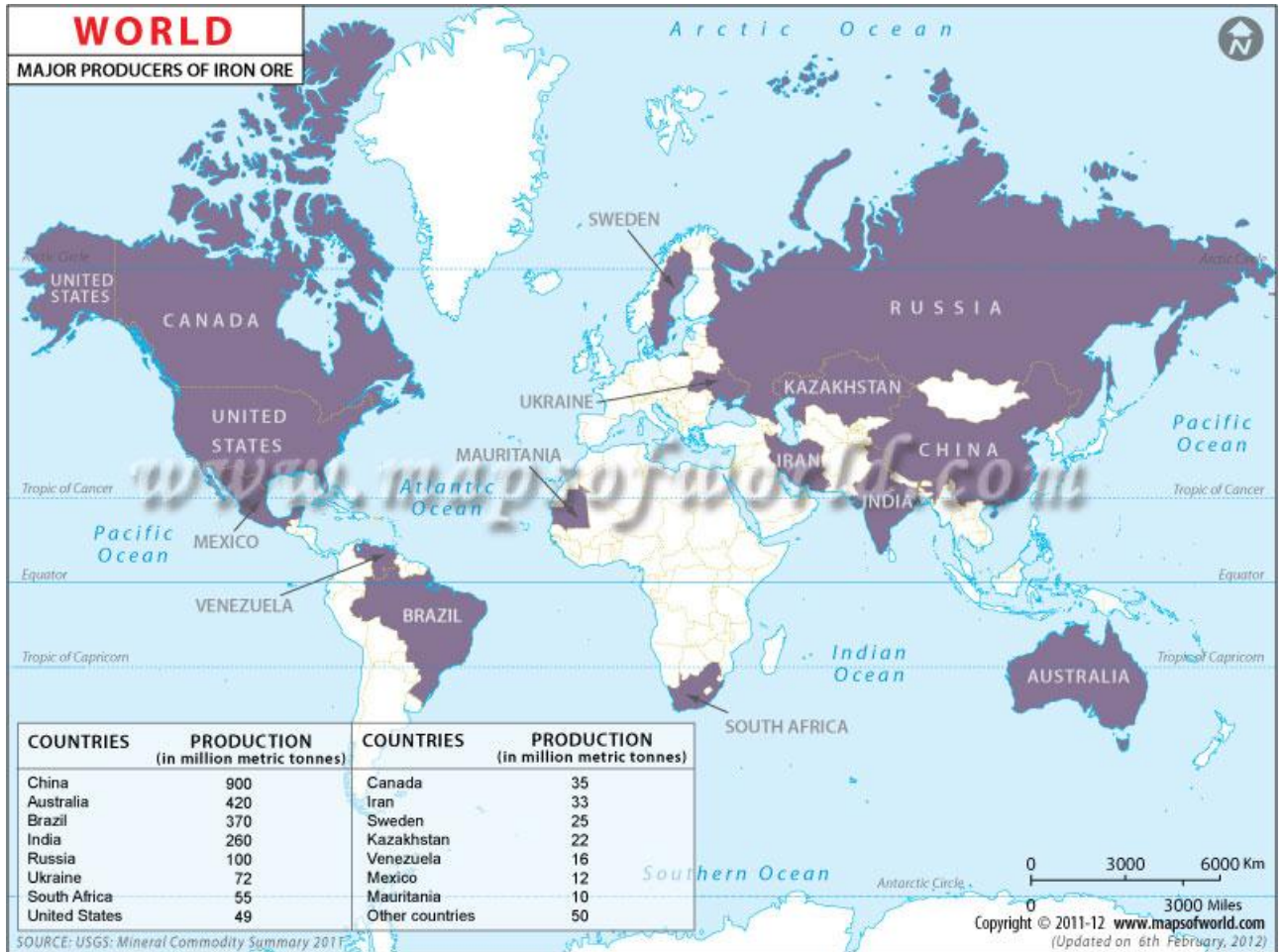
Iron metal is extracted from iron ore, and is almost never found in the free elemental state. Iron is one of the most essential metal to man and all the modern industries are dependent on its supply and availability. Therefore, it is not surprising to find that an iron and steel industry is of basic importance to a country's economic development. In modern times, this heavy industry is rightly considered as index of nation's prosperity, the relative economic strength and powerfulness of a country is reflected in the possession of large and integrated iron and steel works, which is also a measure of the political power and prestige which that country enjoys (Jayanthu et al., 2010).

About 98% of iron ore is used to make steel, one of the greatest inventions and most useful materials ever created . Iron is the most used of all the metals, comprising 95% of all the metal tonnage produced worldwide (Geological Survey of Ethiopia, 2010). Its combination of low cost and high strength make it indispensable, especially in applications like automobiles, the bodies of large ships, and structural components for buildings. Steel is the best known alloy of iron (Brown et al., 2010).

According to the yearly production of iron ore, China, Australia, Brazil, India, Russia, Ukraine, South Africa, Iran, Canada, United States, Kazakhstan, Sweden, Venezuela, Mauritania are the main iron ore production countries in the world (Kirk, 2000) (Fig.1.). The best known and most productive iron deposit in the world explained as a product of magmatic segregation is that of high grade ores at Kiruna in Northern Sweden (Guilbert and

Park, 1986). World resources are estimated to exceed 230 billion tons of iron contained within greater than 800 billion tons of crude ore (USGS, 2013).

World Major Producers of Iron Ore Distribution Map

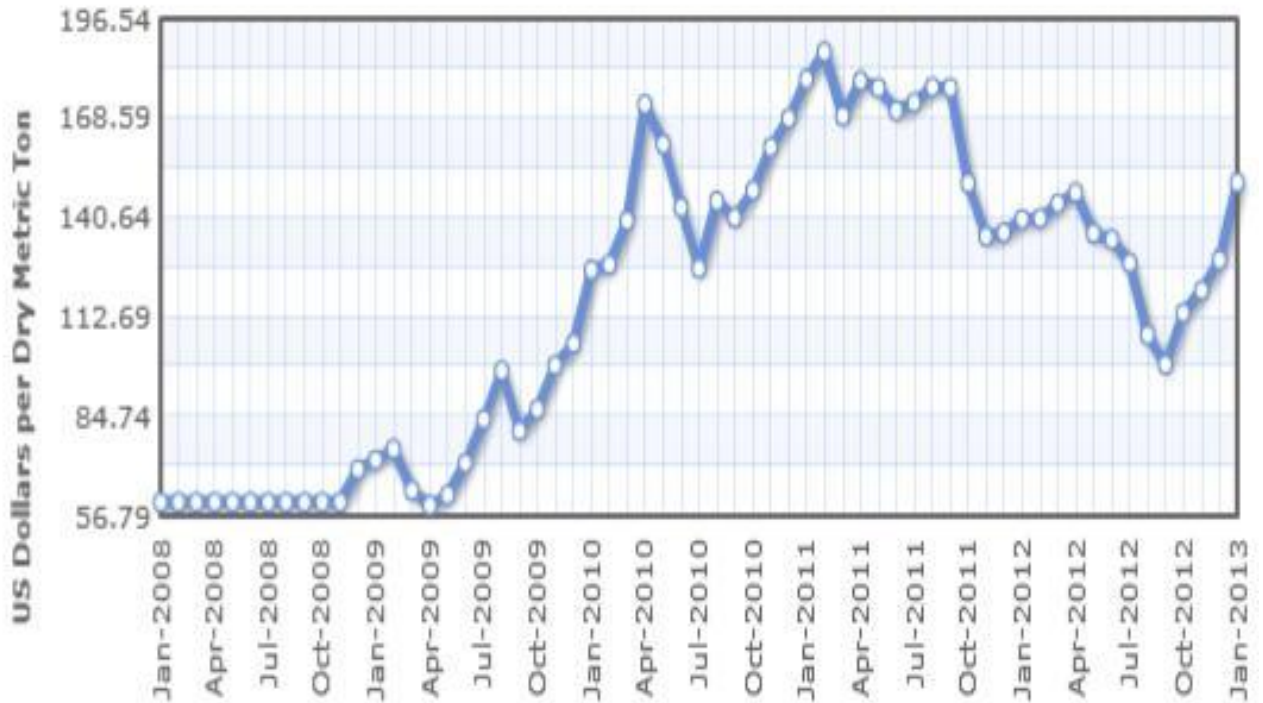


Source: USGS: Mineral commodity summery 2011

Figure.1. World Major Producers of Iron Ore Distribution Map

Iron Ore Price – February 25, 2013:
62.0% Fe Spot CFR Price: US \$153.10/tonne

China Import Iron Ore Fines - 62.0% Fe Spot (CFR) Price



Source: Index Mundi (<http://www.indexmundi.com>)

Figure.2. Iron ore price

1.1. IRON RESOURCES POTENTIAL OF ETHIOPIA

In addition to the big and the first steel industry in Akaki area (Addis Ababa), Currently new steel industry named Toussa Steel Mill project were proposed to erect in Amhara regional state in locality name Combolcha which is expected to be the largest steel mill in Ethiopia with estimated annual production capacity of 1.3 million tons (Addis fortune, 2012).

Iron occurrences were identified in many areas in Ethiopia: among others, Wollega (Gordoma, Chago, Worakalu, Dimma, Billa, and Tulu Bolale) Kaffa (Mai Gudo, Gwmmalucho, Kurkue, Garo, Dombowa, and Melka Sedi), and Tigray (Adua, Enticho) (Tadesse, 2009) (See Appendix II). According to his classification they belong to three main geological settings:

1. Precambrian basic intrusion-hosted Fe-Ti type (Bikilal, Melka Arba),
2. Banded iron formation (BIF) type occurrences associated with Precambrian quartzites (Koree, Gordoma, Chago) and
3. Secondary laterite and/or gossan-related deposits (e.g. Melka Sedi, Garo, Gato, Billa, Gmbo, Gammalucho).

The estimated reserves are: (i) Wollega: Chago (1.2 Mt, 64% Fe), Dha (0.05Mt, 65% Fe), Gordona-Korree (0.27 Mt, 63% Fe), Worakalu (0,15 Mt, 62% Fe), Belowtuist (2.5 Mt), Katta valley (0.1 Mt, 61 % Fe), Yubdo (0.05 Mt, 70.9% Fe); (ii) Kaffa: Garo (12.5 Mt, Melka Sedi (12.5 Mt), Dombova (12.5 Mt), Mai Guda (0.075 Mt, 40% Fe); (iii) Sidamo: Melka Arba (4.63 Mt); (iv) Tigray: Adua, Axum and Enticho (5 Mt, 30% Fe) (EGS, 1989 as cited in Tadesse, 2009).

Other occurrences where total reserves are not yet estimated are found in the following localities: Aim, Famasari, Billa, Gambo, Gmbella- Dembidollo, GeiqDaleti (Wollega), Assale, Beliga, Chilachii Adi Berbere (Tigray), Bissidimo, Galeti, Kunni, Ujau, Soka (Ham), Ghimira Bash, Kurkure, Like (Kaffa) (Tadesse, 2009) (See Appendix II).

The Ethio-Korean Iron Exploration Project reassessed the localities of Dima, Chago, Genji, Koree, Billa, Katta and Bikilal. After two years of reconnaissance work, the exploration team was able to prove the Bikilal area as the major target of exploration. Phase-II activity of the program proved a total ore reserve of 57 million tons of magmatic origin at average grades of 23.3 % magnetic iron and 41 % total iron with the help of drilling and trenching (Ethio-Korean 1988). However, the findings achieved since the early 1960's have not been evaluated and tested for local development of cottage industry (Ethio-Korean Iron Exploration Project, 1988).

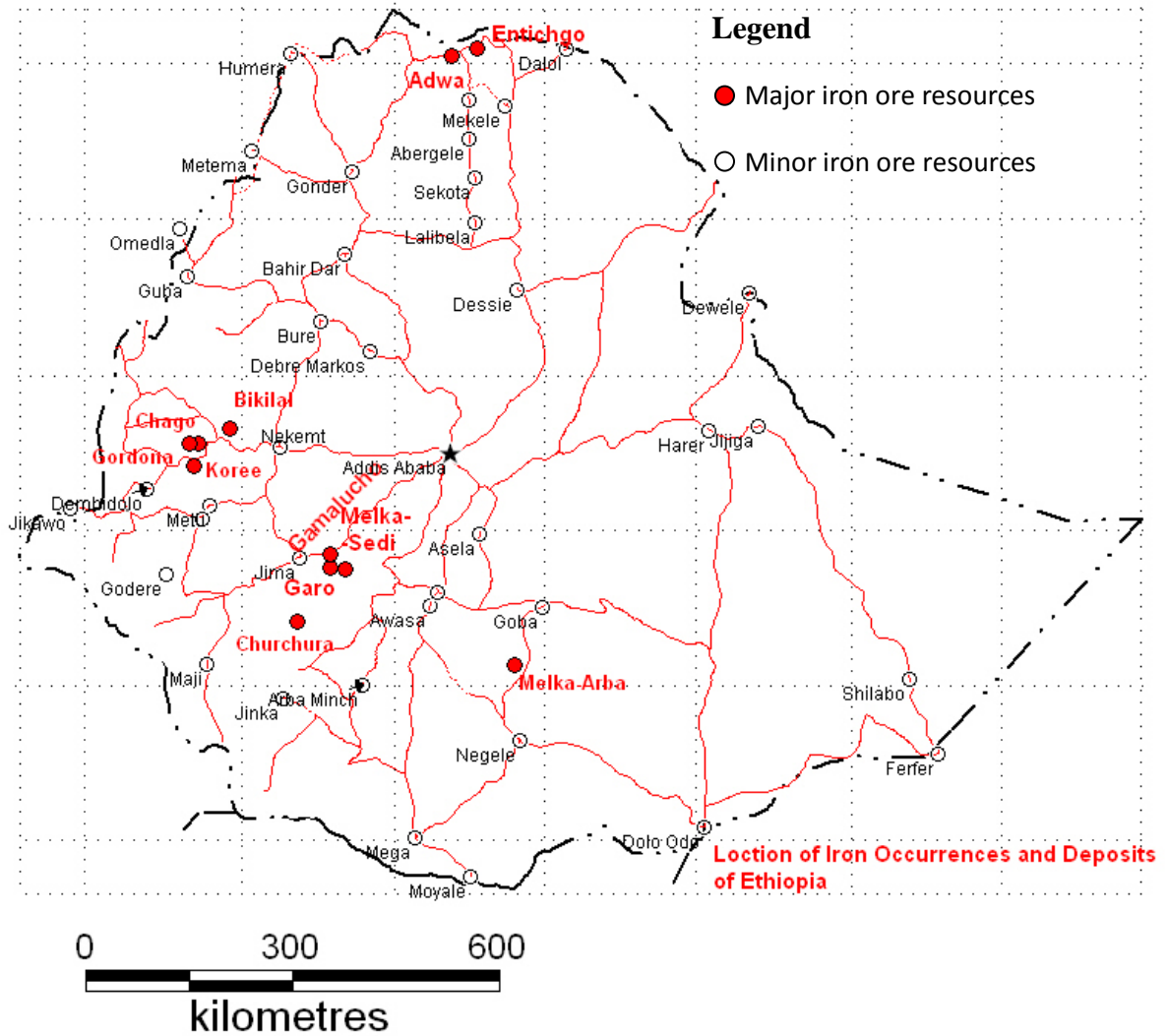


Figure.3. Location Map of Iron Occurrences and Deposits of Ethiopia taken from Geological Survey of Ethiopia, June 2010)

CHAPTER TWO

INTRODUCTION

2.1. LOCATION AND ACCESSIBILITY

Bikilal Iron Deposit is located in West Wollega, Ghimbi zone of Oromia National Regional State, and 440 km west of Addis Ababa. It is found 25-km NNE of Ghimbi town, geographically bounded between $35^{\circ}52'26''\text{E} - 35^{\circ}55'23''\text{E}$, and $9^{\circ}15'15''\text{N} - 9^{\circ}20'6''\text{N}$ and falls in the Ethiopian Mapping Agency topo sheet of No. 0935 D2. This area covers a total area of about 33 Sq. Km.

The study area is reached through Addis Ababa – Ambo-Boku- Sire-Nekemte- and Ghimbi in which mostly the roads are asphalted with some detours and 24 km from Ghimbi town to Bikilal is gravelly road. Beside this, there are foot paths running from the center of Bikilal to Gelel River in the west and Soti River in the East.

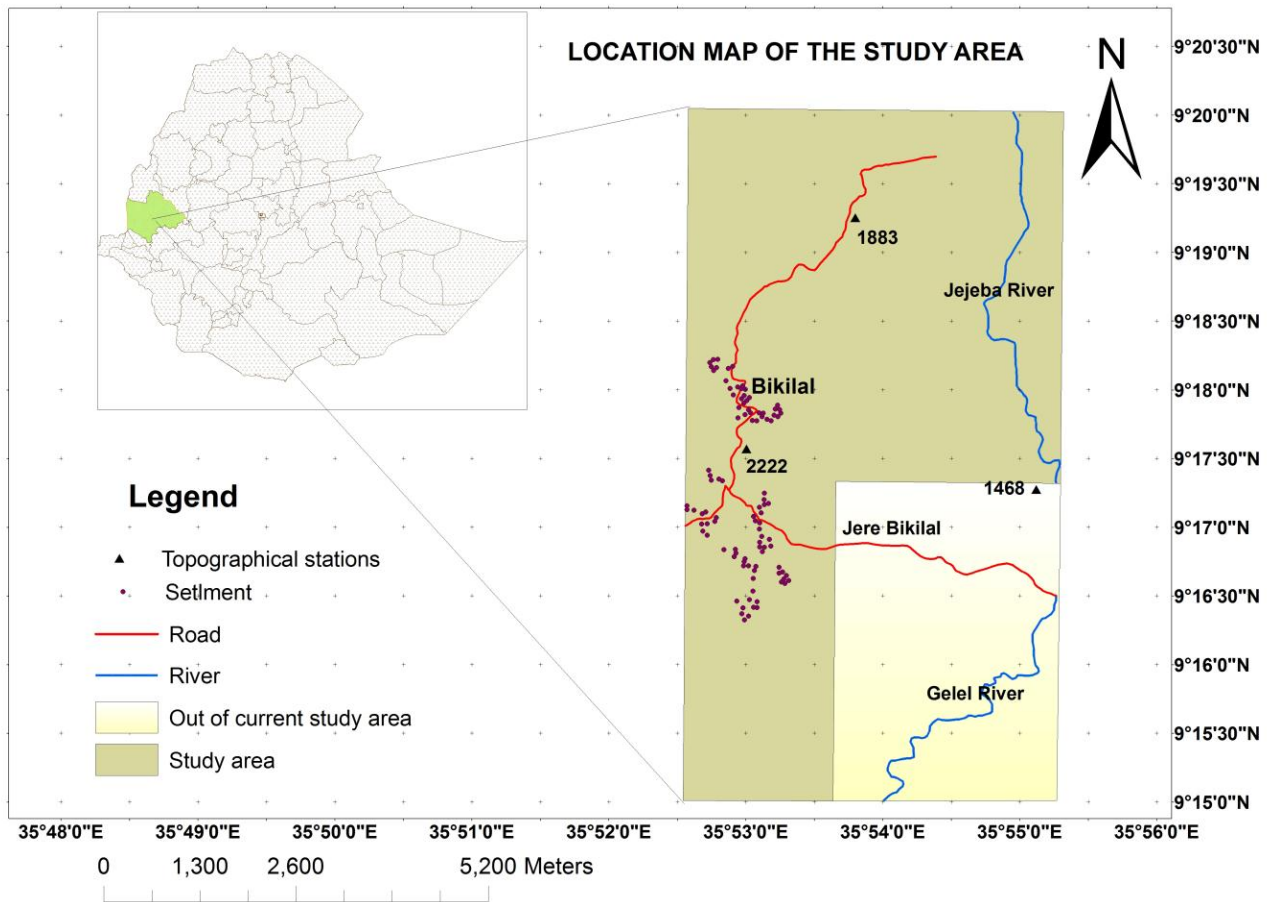


Figure.4. Location Map of the Study Area

2.2. PHYSIOGRAPHY

Physiographically Ethiopia is divided into three distinct units that are the product of major geological evolution of the region.

These are:

1. The Main Ethiopian Rift (MER) and the Afar depression, transect the territory into two and is bounded by steep escarpment and accompanying rift floor that characterized by a series of horst – graben systems. The lowest elevation at Afar depression is 125m below sea level.
2. The North Western Ethiopian plateau and adjacent lowlands, covers more than half of the country, and where the lowlands slope westward into the Sudanese plain.
3. The South – Eastern (Somali) plateau and eastern lowlands. The lowlands include flat plains starting from the Ogaden basin to the east and the Wabi – Shebelle and the Genale plains to the southeast.

Current study area is found within the North Western Ethiopian plateau physiographic unit. Bikilal is a highly rugged and mountainous area. The highest elevation is 2222 m and the lowest elevation recorded in Jejeba river basin is 1200 m. The study area lies between Bikilal mountains and the Jejeba river basin which consists of ridges and valleys. Bikilal is dissected by numerous intermittent and perennial streams which ultimately drain into the main Gelel and soti rivers.

In Gimbi area there are four major rivers. These are Abay, Didesa, Dabus, and Birbir. Dabus and Didesa are the main tributaries of Abay. In the second order there are rivers like Jejeba, Sayi, Soti and Gelel that are tributaries of Didesa. Most of the main streams and rivers follow the N-S, NW -SE, NE-SW and rarely E-W trends. These trends are related to the regional tectonic systems of the Northeast Africa.

2.3. CLIMATE, VEGETATION AND POPULATION

The climate of Ghimbi area generally categorized as Dega (highland), Woynadega, and Kola with average rain fall of 1400- 1800 mm. It has main rainy seasons from May to October and dry season is from December to April 21 with annual temperature of 25⁰ (Ethiopian Central Metrological Agency, Ghimbi Station, 2013). The vegetation cover of the area varies from place to place. Savanna grass, scarce grasses, and long trees with small bushes cover the northern part. The central part is less vegetated and grass covered with long Eucalyptus tree and Tid, but the southern part, is well vegetated with Zigba, Tid, Eucalyptus tree and small bushes with other varieties (Western Wollega, Ghimbi Zone Agriculture and Urban Development Bureau, 2012).

The population of Ghimbi area is estimated to be about 86,340 and in Bikilal Kebele (study area) are about 1758 peoples. Their livelihood depends on agriculture like cultivating coffee primarily, Serial crops (Sorghum, pepper, maize, “chat”) and cattle breeding (Western Wollega, Ghimbi Zone Agriculture and Urban Development Bureau, 2012).

2.4. REVIEW OF PREVIOUS GEOLOGICAL WORKS

The Ethiopia Precambrian rock outcrops in four major areas in the south (Sidamo Province, Gemu- Gofa, Kaffa), in the west (Wollega, Gojam, Begemder), in the north (Eritrea, Tigray) and in the east (Harar) (Mengesha et al., 1996). The high- and low- grade metamorphic terrains of Precambrian rocks of Western Ethiopian rocks are intruded by granitoid with a wide compositional range (Kebede et al., 2001) (Fig. 7). The metamorphic belt consists of high grade biotitic gneisses, low grade volcanogenic sediments, and mafic ultramafic complexes of the Western Ethiopian Shield is an exposed Neoproterozoic metamorphic belt and forms part of the Arabian Nubian Shield (Woldemichael and Kimura, 2008). The reworked Pre-Neoproterozoic and juvenile Neoproterozoic terrain of the Western Ethiopian Shield (WES) comprises of three N–S trending terrains. These are the Western migmatitic gneissic terrain, the central meta-volcano sedimentary terrain (CVST) and the Eastern

migmatitic gneissic terrain. The Eastern part of CVST mostly consists of suture-related ultramafic- metasedimentary complexes, whereas meta-volcanics predominate in the western part. Gabbroic to granitic intrusions are common in the CVST and in adjacent areas (Woldemichael et al., 2010).

Dating conducted on four granitoid places using single-grain zircon Pb/Pb evaporation and conventional U/Pb give time constraints on their emplacement and tectono-thermal events. Magmatic emplacement events were identified for calc-alkaline Ujjukka granite and granodiorite, the anatectic Suqii-Wagga two-mica granite and the Guttin K-feldspar megacrystic granite, and the anorogenic Ganjii monzogranite at 815 Ma, 700 ± 730 Ma, and 620 ± 625 Ma respectively. The 815 Ma age is interpreted to mark a major magmatic episode in this part of Africa (Kebede et al., 2001). In addition new zircon SHRIMP U–Pb ages for two gabbro and three diorites in the Ghimbi-Nedjo region of the Western Ethiopian Shield (WES) showed similar magmatic crystallization ages. Two pulses of magmatism, at 860–850 and 795–785 Ma are documented. By the U/Pb zircon dating ages of 856.3 ± 9.8 and 846.0 ± 7.6 Ma, for the tholeiitic Kemashi diorite and Bikilal Ghimbi Gabbros which have oceanic affinities were known respectively. The mixing of gabbros and diorites with oceanic tholeiitic affinities combined with the new ages suggests that the intrusions were emplaced in the earliest stages of the rifting of Rodinia (Woldemichael et al., 2010). With respect to these events Woldemichael et al. (2010) also suggests that the WES led to the development of a passive margin and associated plume-type magmatism at 855 Ma. The two intrusive groups with differing magma chemistry and ages suggest that the earliest magmatism was tholeiitic and associated with the passive margin system followed by continental breakup to form the Mozambique Ocean. The combination of tholeiitic and calc-alkaline magmatism was related to arc and back-arc basin formation and later terrain accretion (830–690 Ma). The terrain is also associated with mafic–ultramafic belts of suture zones and syn- to post-tectonic gabbroic to granitic intrusions (Fig. 7).

A tectono-thermal event at ~630 Ma preceded the emplacement of the within-plate granitoids at 620 ± 625 Ma. Over a period of 200 million years from the calc-alkaline to anorogenic granitoids which implies a shift of magmatic condition and tectonic setting of the granitoids.

The Suqii-Wagga and Guttin granites, representing the granitoid population in the migmatitic terrain, formed as part of the successive evolution of the granitoid magmatism in the region. The origin and evolution of the granitoids which are emplaced into the low-grade volcano sedimentary sequence and the high grade, often migmatitic, gneisses are due to contribution of pre-Pan-African crust which was evidenced by presence of xenocrystic zircons of Mesoproterozoic ages in both granitoid populations. Conventional U/Pb studies of zircons from the Guttin K-feldspar megacrystic granite and the Ganjii monzogranite yielded upper intercept ages of 3 Ga and 2 Ga, respectively, possibly indicating the presence of reworked Archean-Proterozoic crustal material (Kebede et al., 2001).

Bikilal Ghimbi gabbro is a mafic body surrounded by gneissic rocks consists of fresh and undeformed olivine gabbro in its center and hornblende gabbro and hornblendite with deformational textures at the boundary. According to major element geochemistry despite the differences between the olivine and the hornblende gabbro's, no systematic chemical difference between the litho-types except for the fluid mobile elements, telling an origin from a similar parental magma. Only the boundary is affected by metasomatism. Finally the parental magma composition using the trace element abundance in fresh clinopyroxenes and fresh olivine gabbro bulk rock as intraplate type tholeiitic origin. The intraplate type tholeiitic parental magma suggests plume type magmatism for the origin of the Bikilal Ghimbi gabbro body (Woldemichael and Kimura, 2008).

Bikilal layered gabbro-complex contains olivine/ pyroxene gabbro and hornblende gabbro zones/layers. Repeated lens-like thin and elongated bodies of hornblendite are found closely associated with massive and dispersed magnetite- ilmenite bodies within the hornblende gabbro, in places with apatite (Ghebre, 2010). The outline of elliptical shape of Bikilal-Ghimbi gabbroic complex is measuring 42 km in length and 3.5 to 11km in width and forms the elongated Bikilal-Gimbi-Chuta-Keki mountain range. The complex is situated east of the Tulu Dimtu mafic-Ultramafic belt, and appears to have an intrusive contact with the rocks of the Aba Sina domain. Large part of gabbro is mostly composed of amphibole gabbro, olivine gabbro with minor leucogabbro, anorthosite, hornblendite and ultramafic (Alemu and Abebe, 2000).

Based on the petrological analysis the Bikilal layered gabbro complex contains hornblende, plagioclase, opaque minerals/ ilmenite + magnetite, and apatite were found within the hornblende gabbro and that of hornblendite shows hornblende, apatite, ilmenite and rare sulphides, and traces of Uranium (Ghebre, 2010). The complex is divided into marginal and middle zone. The peripheral zone consists of melanocratic gabbro, which is generally fine-grained, but coarsens towards the interior of the intrusion and exhibits hypidiomorphic texture. The middle zone is the broadest one and consists of gabbro with minor Anorthosite and hornblendite. The middle zone is characterized by very well defined layering vary from meter dimensions to centimeters to single crystal thickness and dip of layers are nearly vertical (70-90⁰) (Alemu and Abebe, 2000).

The Bikilal Precambrian rocks consisting of biotite and/or granitic gneiss, metahornblendite gabbro, apatite- iron bearing metahornblendite, granite, olivine- gabbro, and granite and pegmatite dikes. Of this biotite and/or granitic gneiss, metahornblendite gabbro, apatite- iron bearing metahornblendite are metamorphosed from upper greenschist through lower amphibolite to medium amphibolite facies (Beshawered, 2001). The oldest unit, biotite and / or granitic gneiss has encountered one-phase of deformation and shows meso-scale sinistral shear zone in the northern portion of the map area, suggesting the presence of a big shear zone, possibly of Didessa Shear Zone (DSZ). The Bikilal basic ultrabasic rocks are alkaline to subalkaline magmas of tholeiitic affinity. This basic ultrabasic intrusive complex comprises two types of deposits: massive (ilmenite + magnetite) and disseminated (apatite-ilmenite-magnetite) ores. Both deposits are prominently confined to thin lenticular bodies of apatite-magnetite-ilmenite bearing metahornblendite and metahornblende gabbro. Finally he suggests that these deposits are the result of late- stage differentiation of basic magma that is emplaced along "weak" zones. In addition to this, the presence of apatite in oxides, pyroxene, and/or hornblende might suggest that liquid immiscibility might have played a vital role in their formation (Beshawered, 2001).

In Bikilal iron ore deposit, Ethio- Korea Iron Ore Exploration Project was accompanied in two phases; the first phase was conducted in 1986. In this phase Ethio-Korean Company aimed to see the governing geologic conditions and host rock property of the iron mineralization in the area, to outline the extent and shape of the Bikilal titanite- magnetite deposit, investigating the mineral constitutions, to investigate the industrial (technological) or beneficiation property of the ore, and finally to determine the dimension and to estimate the reserve. The length of the ore bearing zone was estimated to be 15 Km and the actual length and width of the iron ore bodies are 4.9 Km and 40 – 60 meters respectively. From the drilling data the vertical thickness of the ore body was found to be 200 meters. During this phase of exploration work the iron ore reserve in this area was estimated to be about 18,000,000 tons with an average of 44% iron grade from 40 different ore bodies (Ethio-Korean Iron Exploration Project, 1986). The detailed geological survey which carried out over this ore zone was trenches, pits and boreholes.

In addition to the types of activities which were done in the first phase of exploration this company conducted its work for the second time in 1988 after two years and re estimates the reserve to be about 57,800,000t based on 10000ms trenching and 13056m (54 boreholes) of subsurface prospecting in advance that of the former estimation (Ethio-Korean Iron Exploration Project, 1986)

2.5. OBJECTIVE

2.5.1. GENERAL OBJECTIVE

The main objectives of the study are to investigate the structures, petrology and the different alterations within the mineralized zone of Bikilal in attempt to reveal possible factors responsible for their evolution and distribution patterns with respect to Iron mineralization and its association with sulfide and gold mineralization. Moreover, the general geological characteristics of the already discovered Bikilal iron deposit, like morphology of the ore deposit, host rock lithology and metal associations of the ore deposit is to be determined and synthesized.

2.5.2. SPECIFIC OBJECTIVES

The specific objectives of this paper are:

1. Describing the ore forming processes and alteration of the mineralized zone.
2. To study and determine the textural and grain to grain boundary characteristics under microscope
3. To study the mineralization and paragenetic sequence of the ore and gangue
4. To understand geological host material of the iron and its mineral association.

2.6. METHODOLOGY

To achieve the specific and general objective of this study the following methods and approaches were adopted.

2.6.1. SECONDARY DATA COLLECTION AND INTERPRETATION

Topographic maps, published and unpublished reports, journals, field manuals, established data related to the present study were collected from different sources and made basis for the field investigation. Several geological maps produced by Ethio-Korea Exploration project and Geological Survey of Ethiopia at different scales were also extensively used to locate different exploratory works (trenches, pits, and boreholes) and to understand the geology better. Aerial photos were used for the interpretation of tectonic lineaments.

2.6.2. FIELD WORK

The field work mainly consists of field mapping which was carried out by route mapping on 1:50,000 scale topographic maps. Geological traverses were made mainly on the roads, river cuts and foot trails. For lithological and petrographical characterization about 20 rock samples were collected. Several measurements of structural elements are recorded, mainly around the main mineralized bodies.

2.6.3. PETROGRAPHY

Petrographic investigation on selected representative rock samples have been conducted in view of understanding the mineral types, association, texture, deformation, alteration and metamorphism. From those different trench and surface chip rock representative samples about 20 samples were selected for extra petrographic description and examinations under microscope. 10 samples each for thin section and polished section were prepared to determine and describe the respective mineral assemblages, their association and inspect any interesting features. The petrographic sections were prepared in the Geological Survey of Ethiopia central laboratory. In addition, field information was compiled in GIS using Arc-GIS software to generate geological map of the area and iron mineral occurrence and distribution zone. Finally, by integrating the pre-field, during field and post-field works a large scale geological map of the area at scale of 1:25,000 were produced.

CHAPTER THREE

REGIONAL GEOLOGY

3.1. EAST AFRICAN OROGONY

Approximately one-third of Earth's surface is covered by continental crust (Bowring and Williams, 1999 as cited in Stern and Scholl, 2010). The assembly of Eastern part of Gondwana (Eastern Africa, Arabian–Nubian Shield, Seychelles, India, Madagascar, Sri Lanka, East Antarctica and Australia) resulted from a complex series of orogenic events spanning the interval from ~950 to ~530 Ma. Detailed examination of the geochronologic database from key cratonic elements in Eastern Gondwana suggests a multiphase assembly (Meert, 2002).

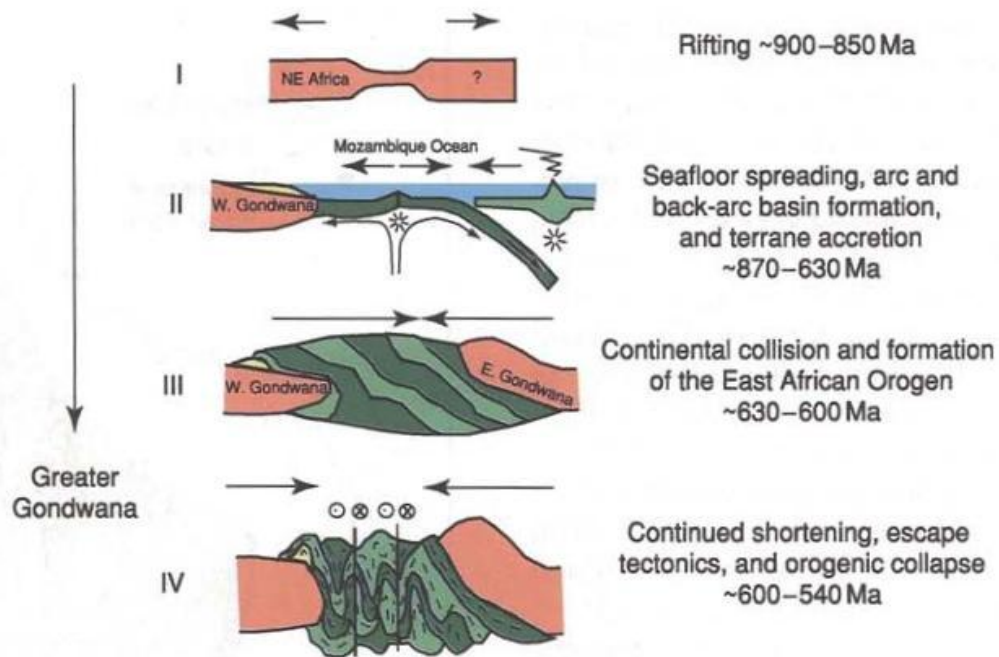


Figure.5. The suggested evolution of the Arabian–Nubian Shield after Kröner and Stern, 2004.

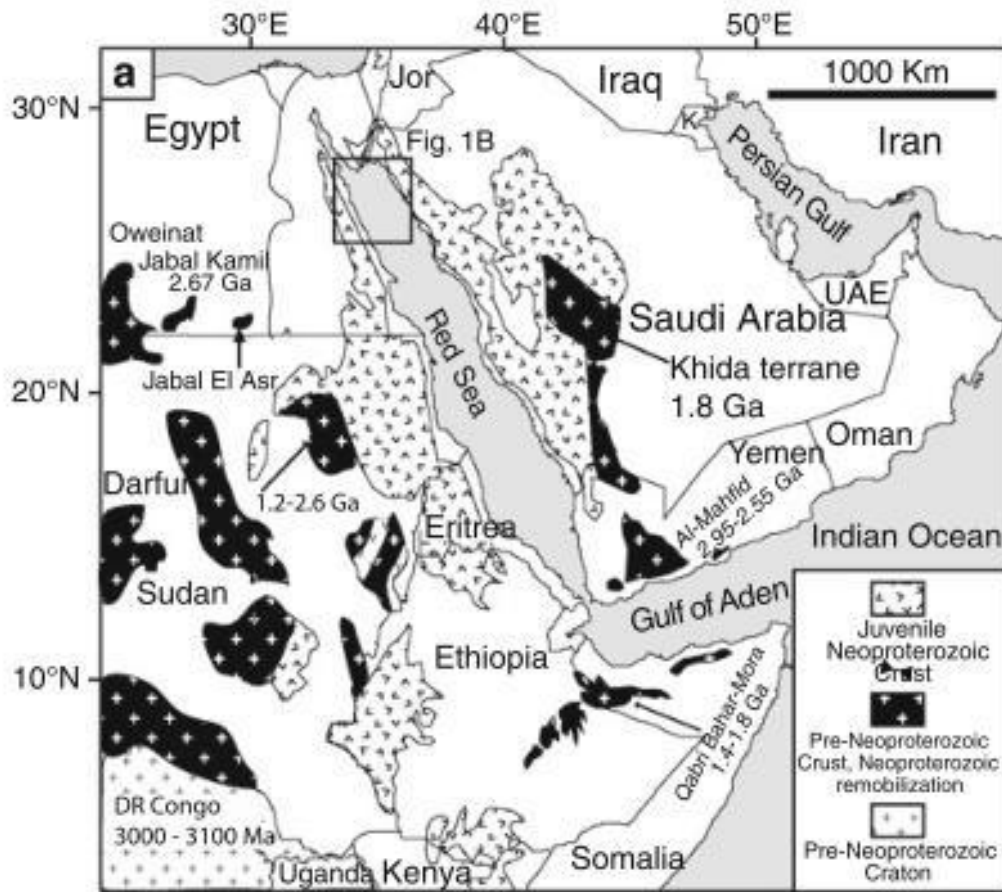


Figure.6. Map of the Arabian–Nubian Shield (Modified from Stern et al. 2006), showing the location of the study areas and regions where pre-Neoproterozoic crust is found.

The term Pan-African originally referred to a sequence of tectono-thermal events at 500 ± 100 Ma within Africa and Gondwana (Kennedy, 1964 as cited in Stern, 1994). The presence of a widespread phase of extension at the end of the Pan-African period in the Arabian–Nubian Shield requires a new interpretation of the tectonic history of this shield. Different tectonic phases are recognized in the Late Proterozoic of the Arabian–Nubian Shield. Ophiolites and island-arc remnants are relicts of an oceanic phase, the oldest one. This phase was followed by arc-accretion, well established in the Arabian–Nubian Shield from the presence of individual terrains bordered by sutures, which was responsible for lithospheric thickening (Blasband et al., 2000).

The Pan African belt system displays evidence of complex crustal evolution which took place in several phases during the period of 1100 Ma to about 450 Ma ago. Some belts clearly indicate that modern-type plate tectonic processes were already at work in the late Precambrian, while other regions suggest a development not involving plate separation and subduction of oceanic crust. If this is correct, the Pan African may represent a tectonic regime transitional between predominantly intra-plate deformation of the older Precambrian and predominantly plate margin deformation of the Phanerozoic type (Gaudette and Hurley, 1979).

The generalized application of Wilson-Cycle models as proposed for Phanerozoic collision belts may perhaps not be justified in view of the increasing evidence favoring non-uniformitarian crustal evolution through time. This is not to say that plate tectonics did not operate during the Precambrian, but it is likely that somewhat different plate interaction at that time produced different effects in the rocks that we now see, and the excellent exposures in some Pan African terrains should enable us to decipher this process (Kröner, 1980).

Kennedy (1964) clearly meant to specify the entire structural differentiation of an original shield into orogenic areas and, according to present data, this started between 1100 Ma and 1000 Ma ago. In this sense, the Pan African constitutes one of the major crust-forming events of earth history, and the term should therefore be applied accordingly. Individual episodes of the Pan African should be named after the areas in which they are observed, as, for example,

the Damara, Katanga, and Pharusian episodes. It may eventually also become advisable to extend the term to other Gondwana continents or to devise a new name that could be applied to all these regions (Kröner, 1980).

The Saharan Metacraton is dominated by medium to high-grade gneisses, meta-sediments, migmatites, and smaller outcrops of granulite, but low-grade volcano-sedimentary rocks are not uncommon. These metamorphic rocks are intruded by Neoproterozoic granitoid ranging in age between 750 and 550 Ma. The medium to high-grade metamorphism suggests that these terrains could be Pre-Neoproterozoic continental crust, but Rb/ Sr and U/Pb zircon age determinations indicate that some, maybe most, of these gneisses were formed and/or metamorphosed during Neoproterozoic time (Abdelsalam et al., 2002).

3.2. WESTERN ETHIOPIAN SHIELD

The Ethiopian Precambrian basement was traditionally classified into three complexes (Asrat et al., 2001). The lower complex formed of high grade gneisses represents older (older than 2500 m.y.) cratonic basement. The middle complex (clastic meta-sediments) is presumably the Lower to Middle Proterozoic platform cover. The upper complex consists of low-grade rocks in following succession: ophiolitic rocks, andesitic meta-volcanics and associated meta-sediments, clastic and to less extent carbonate sediments (Kazmin et al., 1978). Later these traditional classifications were revised based on the recent geochronological, thermochronological, geochemical and lithotectonic data (Asrat et al., 2001).

Western Ethiopian Shield is an exposed Neoproterozoic metamorphic belt and forms part of the Arabian Nubian Shield. The metamorphic belt consists of high grade biotite gneisses, low grade volcanogenic sediments, and mafic ultramafic complexes (Woldemichael and Kimura, 2008). The Western Ethiopian Shield (WES) lies near the transition between the ANS and the Mozambique belt, and also lies adjacent to the enigmatic “East Saharan Metacraton”, which consists of older crust that was extensively remobilized during Neoproterozoic time (Abdelsalam et al., 2002).

Precambrian of Western Ethiopia consists of high grade gneiss and migmatites in the east and west and low grade meta-volcanic sedimentary rocks at the center which are bounded in either sided by two parallel NNE-SSW trending ophiolitic belts (Tulu Dimtu and Assosa Kurmuk) (Alemu and Abebe, 2000).

Western Ethiopia basement divided into five units from east to west these are: eastern block of high- grade Pre- Pan- African rocks (zone 1), ophiolite belt (zone 2), zone of diorite-granodioritic batholiths and associated intermediate volcanics (zone 3), meta-volcanic meta-sedimentary belt (zone 4) and western block of high grade Pre-Pan-African basement (zone 5 (kazmin et al., 1978) (Fig.7.). In addition to this Kebede and Koeberl (2002) subdivided the Western Ethiopian Precambrian rocks into two contrasting groups, namely the high-grade gneissic terrain and low-grade volcano-sedimentary terrain. The lithological boundary between the terrains is tectonic, as marked by ultra-mylonitic rocks. The high-grade terrain lies west (along the Sudanese border) and east of the low-grade belt. Towards south the migmatitic gneisses become more important and grade into Mozambique belt rocks of Kenya. In contrast, in Northern Ethiopia and Eritrea only the low-grade assemblages, without bordering migmatitic gneisses, are found. The low-grade volcano-sedimentary sequences characteristically contain mafic-ultramafic rocks which are considered to represent ophiolites. These generally greenschist facies rock assemblages, with their attendant dismembered ophiolitic rocks, as exposed in Sudan, western and southern Ethiopia represent the southern extension of the Arabian Nubian Shield (ANS).

Woldemichael et al. (2009) suggests two major crustal types are identified in the East Africa –Antarctic Orogeny (EAAO). The juvenile (i.e., mantle derived) ANS in the north is dominated by low-grade volcano-sedimentary rocks in association with plutons and ophiolitic remnants. The second crustal type is a tract of older remobilized crust to the south of the ANS, known as the Mozambique Belt (MB). The transition between the juvenile ANS and MB is located within Ethiopia, Eritrea, Sudan and Somalia. The WES lies near the transition between ANS and MB, and also adjacent to the “East Saharan Metacraton”, which consists of older crust that was extensively remobilized during the Neoproterozoic time (Abdelsalam et al. 2002). Several lithological and structurally distinct domains are

recognized within the WES. Studies of the geochronology and the geochemistry of WES plutonic rocks are limited and are based mainly on granitic rocks.

Three generations of plutonism are recognized in the WES these are “pre-kinematic” (830–810 Ma) and “syn-kinematic” plutons (780–700 Ma) were subduction related, emplaced in intra-oceanic island-arc environments. The late- and post-kinematic plutons (620–550 Ma) are considered to represent both subduction-related and intra-plate post-collision intrusions. There is no evidence that WES igneous activity occurred prior to any EAAO tectonic event, although the age and affinity of poly deformed gneisses and most WES intrusions were not well studied (Kebede et al. 1999; 2001).

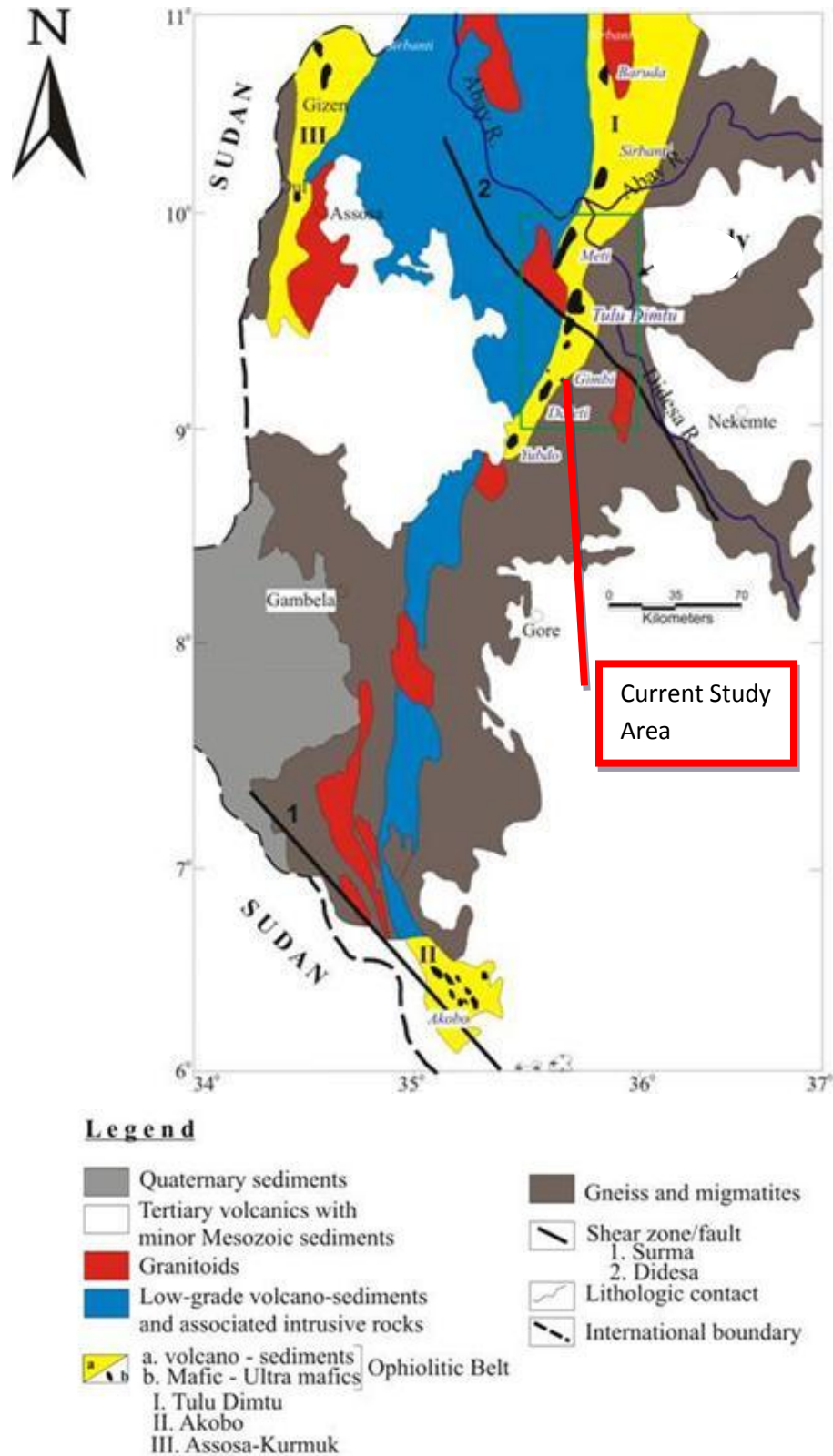


Figure.7. Simplified geological map of the Precambrian of Western Ethiopia (modified after, Mengesha et al., 1996 by Tadesse and Tsegaye, 2000).

CHAPTER FOUR

GEOLOGY OF BIKILAL AREA

Bikilal intrusions are segment of the Pan-African Orogeny of the Mozambique Belt, which is underlain by Precambrian rocks dominantly composed of gneiss; that is intruded by mafic to ultramafic rocks (Woldemichael and Kimura, 2008). The latter is cut by small scale localized granite, and pegmatite dikes at various places within the area. Bikilal Gabbro complex has an elliptical shape and covers an area of about 350km² (Ghebre, 2010). Bikilal Ghimbi gabbroic intrusion exhibits sheared intrusive contact against the adjacent Precambrian gneiss. The Precambrian rocks comprise mainly granite, meta-diorites, schist, meta-sediments and amphibolites. In Bikilal-Ghimbi intrusive complex three major and other minor lithological units were identified. The major lithological units are olivine gabbro, hornblende gabbro and hornblendite while pegmatite, granite, migmatite, and anorthosite are minor lithological units (Woldemichael and Kimura, 2008).

Mafic–ultramafic intrusions commonly display prominent petrographic and geochemical layering attributed to differentiation in a magma chamber. This layering occurs at scales from several hundreds of meters in some large intrusions, down to scales of a few millimeters. Individual layers or layered sequences can vary greatly in thickness, texture, shape, and in their mineralogical and chemical composition (Ferré et al., 2009); the Bikilal-Ghimbi intrusion is no exception. The olivine gabbro body has no clear layering. However, an intensive layering is only limited in the periphery, which mostly consists of hornblendites and hornblende gabbros, whereas the olivine gabbro cores are apparently massive. Layering/banding features occur in the hornblende gabbro.

Bikilal gabbroic intrusive complex consists of olivine gabbro in the center and hornblende gabbro, anorthosite and hornblendites at the periphery. The optical properties of minerals and their textural relationships have been studied using a polarizing microscope. Description of each lithological unit supported by petrological examination, hand specimen and field mapping is discussed as follows:

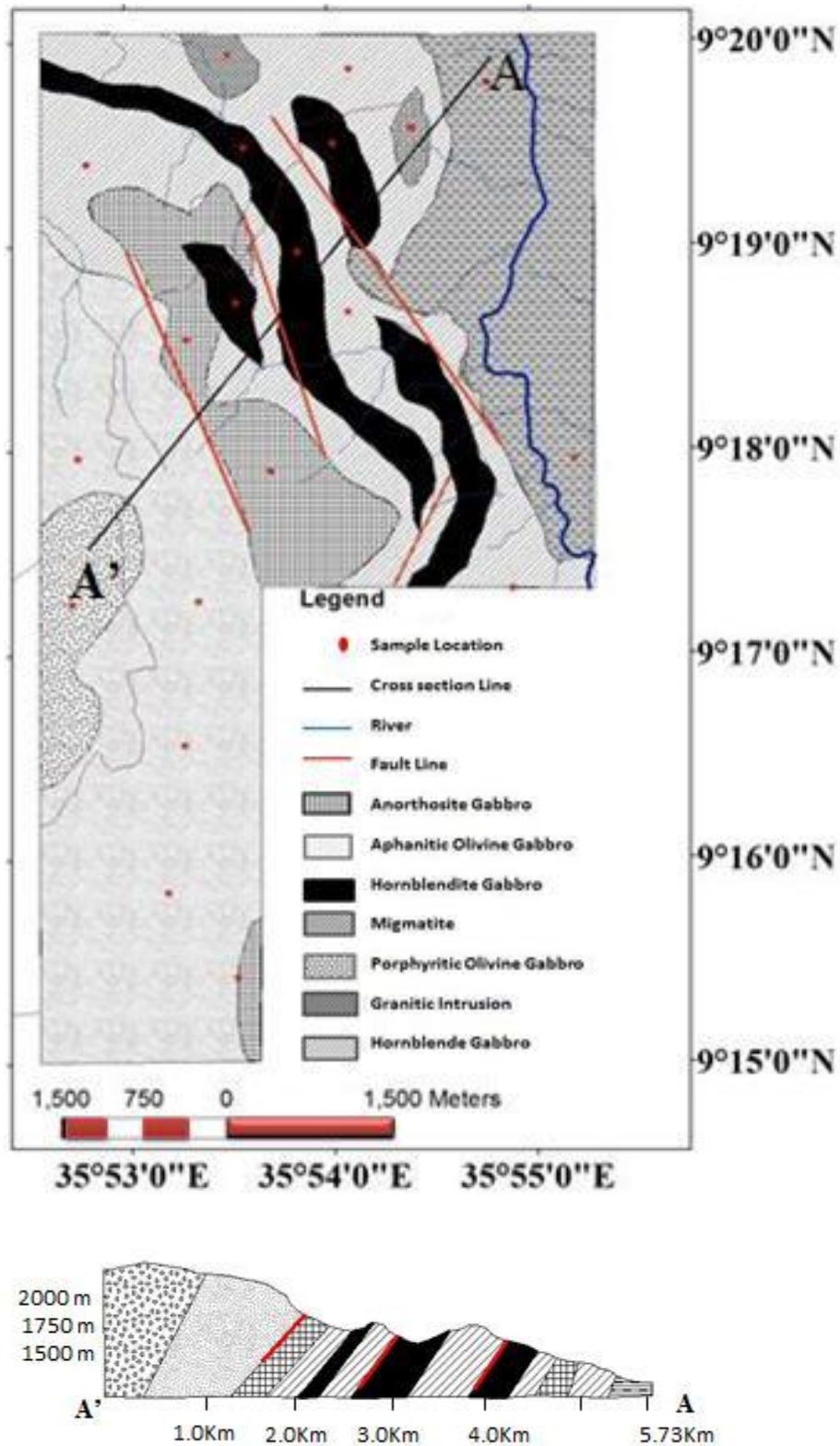


Figure.8. Geological map and cross section of Bikilal intrusive gabbro

4.1. PORPHYRITIC OLIVINE GABBRO

This rock unit is extensively occupies the central portion of the intrusion with massive to rarely porphyritic in texture. It gradually grades in to aphanitic olivine gabbro as one move's away from the center. The rock is dark in color and medium to coarse grained texture. Based on petrographic examination of this unit the following mineral compositions were identified: olivine 25- 30%, pyroxene 4- 7%, plagioclase 30- 35%, apatite 0- 15%, opaque 7- 12% (ilmenite + magnetite + sulphides), and with trace amount of biotite minerals. It is green to dark grey in color and course to medium grained texture of size range from 2 to 5mm with subhedral to anhedral shape. Olivine mineral grains are randomly distributed sometimes found in the plagioclase as a xenoblast texture. Plagioclase has a subhedral to anhedral very elongated sometimes rounded in shape with a size range from 1.5- 6 mm in its width and 7mm- 8cm in its length. Anhedral to subhedral opaque minerals were also found as inclusion in the olivine and plagioclase as xenoblastic texture with size ranges from 0.5- 3 mm. All the crystals are weakly zoned and they are not fractured (Fig.14 (A &B)).

4.2. APHANITIC OLIVINE GABBRO

The aphanitic olivine gabbro extends north-south direction in contact with the anorthosite along the edge of the porphyritic gabbro. This rock is exposed more widely at the extreme north and south tips of the porphyritic olivine gabbro. Small scale irregular shaped aphanitic olivine gabbro occurs inside the anorthosite. Xenoliths of porphyritic olivine gabbro are also found scattered in the aphanitic olivine gabbro. The aphanitic olivine gabbro is fresh and unaltered, except for minor veins and weathering. Deformation textures are rare, and all the crystals are fresh and retained their original shape.

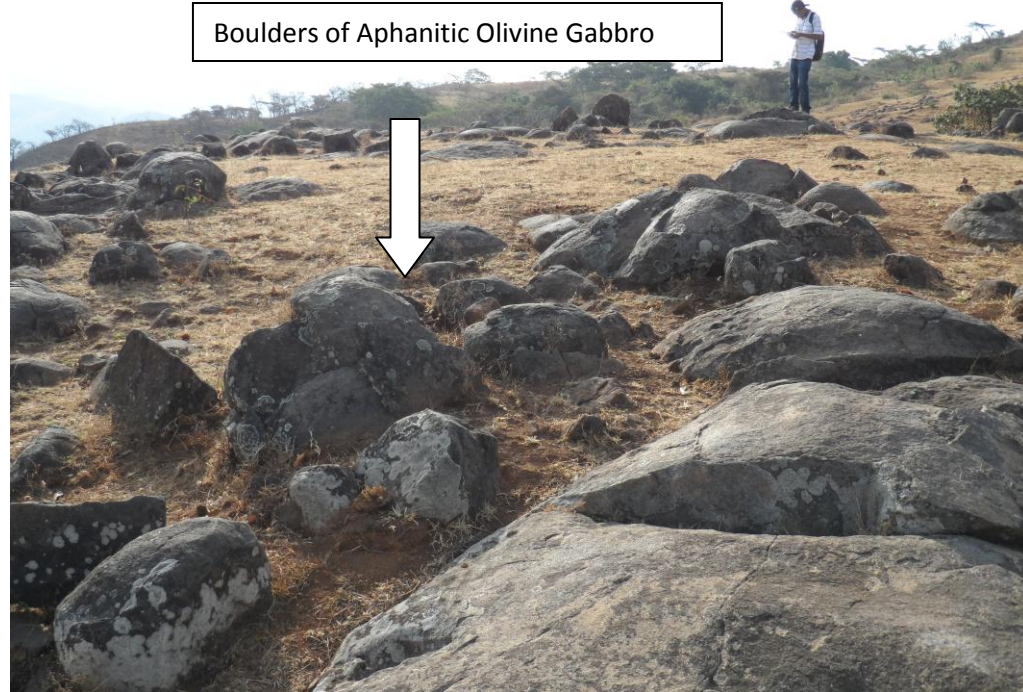


Figure 9. Field photo of Aphanitic Olivine Gabbro

4.3. HORNBLLENDE GABBRO

Hornblende gabbro units are found at the periphery of the intrusion and form large portion of it. The rock in this unit is characterized by melanocratic to leucocratic varieties, depending on the plagioclase and hornblende content, and generally medium to coarse grained texture. It has greenish grey to dark greenish grey appearance under microscope. Coarser and finer varieties of these units were observed; generally medium grained with an average grain size of 3-4mm. Within the hornblende gabbro, repeated lens-like thin and elongated horizons of hornblendite are found intimately associated with massive and disseminated magnetite-ilmenite in places with apatite ore bodies.

Plagioclase and hornblende exhibit a relict to granoblastic texture, with accessory ilmenite, apatite, and chlorite. Petrographical examination shows that the hornblende gabbro is composed of 45-55% hornblende, 6-10% (opaque) ilmenite + magnetite + sulphides, 20-

25% plagioclase, 3- 6% apatite, and 3-4 sphene with a dominant subhedral – anhedral texture. The matrix composed of hornblende and plagioclase is showing alignment of schistosity (Fig.15 (B)), opaque minerals are rimed by sphene. The plagioclase shows fine lamellar twinning and a fold structure developed within the crystals, indicating that the rocks had undergone deformation. In a few places, plagioclase shows a granular texture and is broken down to form fine grains, from which the original twinning is lost. These observations, combined with the gradational contact with the olivine gabbros seen in some places, suggest metasomatism at late stage magmatism may have played a role in the formation of the hornblende gabbro.



Figure 10. outcrop photo of Hornblende Gabbro along trench

4.4. HORNBLENDITE GABBRO

Hornblendite is exposed mostly inside the amphibole rich anorthosite and in hornblende gabbro. The hornblendite occurs as an elongated lenticular body having an irregular curved line shape. The strike extension of the hornblendite range from tens to hundreds of meters and the width varies from some meters to tens of meters. Magnetite- ilmenite ore body is present in this rock unit either in disseminated or massive form.

Hornblendite rocks are deformed and have medium to very coarse-grained texture with light green to dark green appearance under microscope. Hornblende grains are subhedral to anhedral in shape. Petrographic examination reveals hornblendite shows 75 to 80% hornblende, 10 - 12% opaque (ilmenite + magnetite + sulphides), 8- 10 % plagioclase, 2- 4% apatite, with minor pyroxene, biotite, quartz and chlorite as retrograde mineral. Hornblendite units are hosted within the hornblende gabbro and anorthosite gabbro. Hornblende minerals are the dominant phase in this unit with a grain size ranges from 1.5- 4.5mm. Opaque grains are found as a xenoblast inside the hornblende and sometimes aligned alongside. The hornblende and plagioclase grains in this unit show the schistose alignment along a specific deformation direction in response to the shearing of the intrusion with the surrounding Precambrian gneiss.



Figure 11. Field photo of Hornblendite Gabbro

4.5. GRANITE AND PEGMATITE DIKES

Granite dikes are found within hornblende gabbro at the periphery of the intrusion. Besides, pegmatite dikes are also seen in association with the granitic dikes and hornblende gabbro with an average thickness ranging from few centimeters to half a meter and visible length of 10-15 meters. Pegmatitic veins are intersected by drilling (Consult 4 International, 2001). They are dull – white and coarse grained with a grain size of 5 – 6mm and composed of quartz, plagioclase and muscovite. The thickness of pegmatite veins intersected is not usually greater than 10m (Ghebre, 2010).

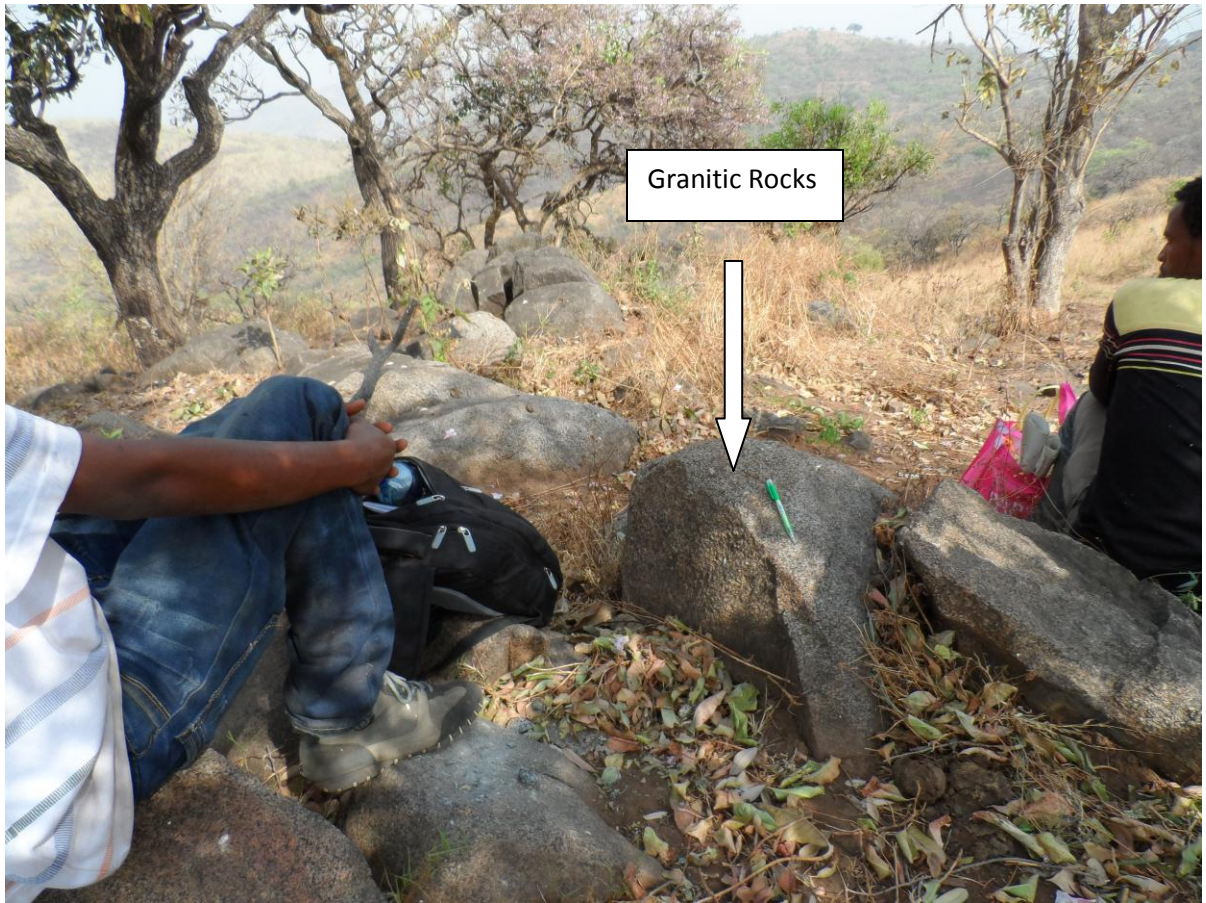


Figure 12. Field photo of granitic intrusion

4.6. ANORTHOSITE GABBRO

This unit is encountered as patches within the hornblende gabbro unit, at the eastern side of the olivine gabbro and it is the smallest of all units. Anorthosite is observed as thin layers measuring from few centimeters up to meters in thickness, and represents the upper part of the middle zone. They are gray to light gray in color, medium to coarse grained and composed of entirely plagioclase with minor amounts of amphibole with opaque minerals. The anorthosite group appears as rim shape at some places. It has an aerial coverage of 1-2.5km x 20 km along the north-east and north-west outskirts of the Bikilal intrusion (Ethio-Korea, 1986).



Figure 13. Field photo of Anorthosite gabbro

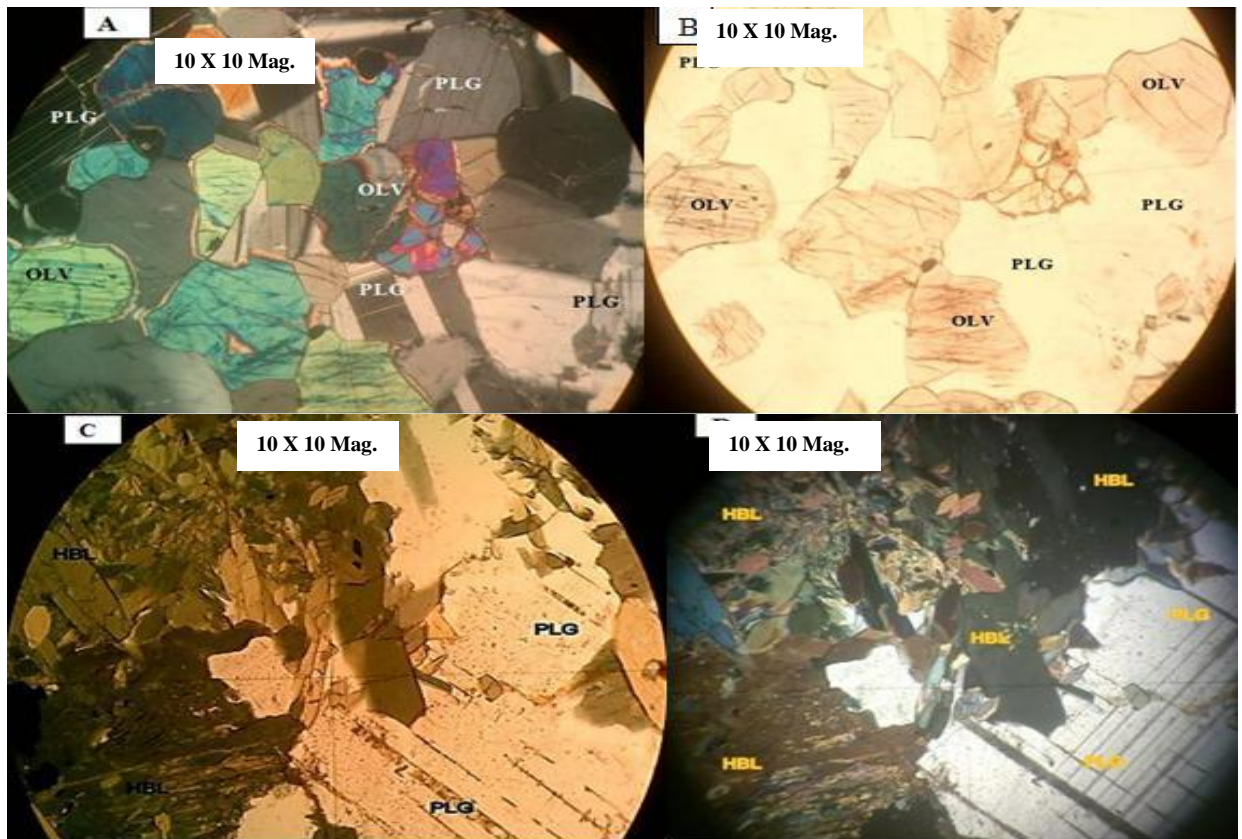


Figure.14. Photomicrographs of gabbro showing different rock forming minerals and opaque mineral association (A) Olivine gabbro under xpl with olivine (OLV), plagioclase (PLG) and hornblende (HBL) association with in the olivine gabbro is under crossed polarized light (B) is olivine gabbro under plane polarized light. (C&D) shows a plane and crossed polar view of a hornblende and plagioclase mineral association and in this section there are trace amounts of chlorite and biotite in addition to this the plagioclase twin lamella shows a curve appearance due to deformation in hornblende gabbro.

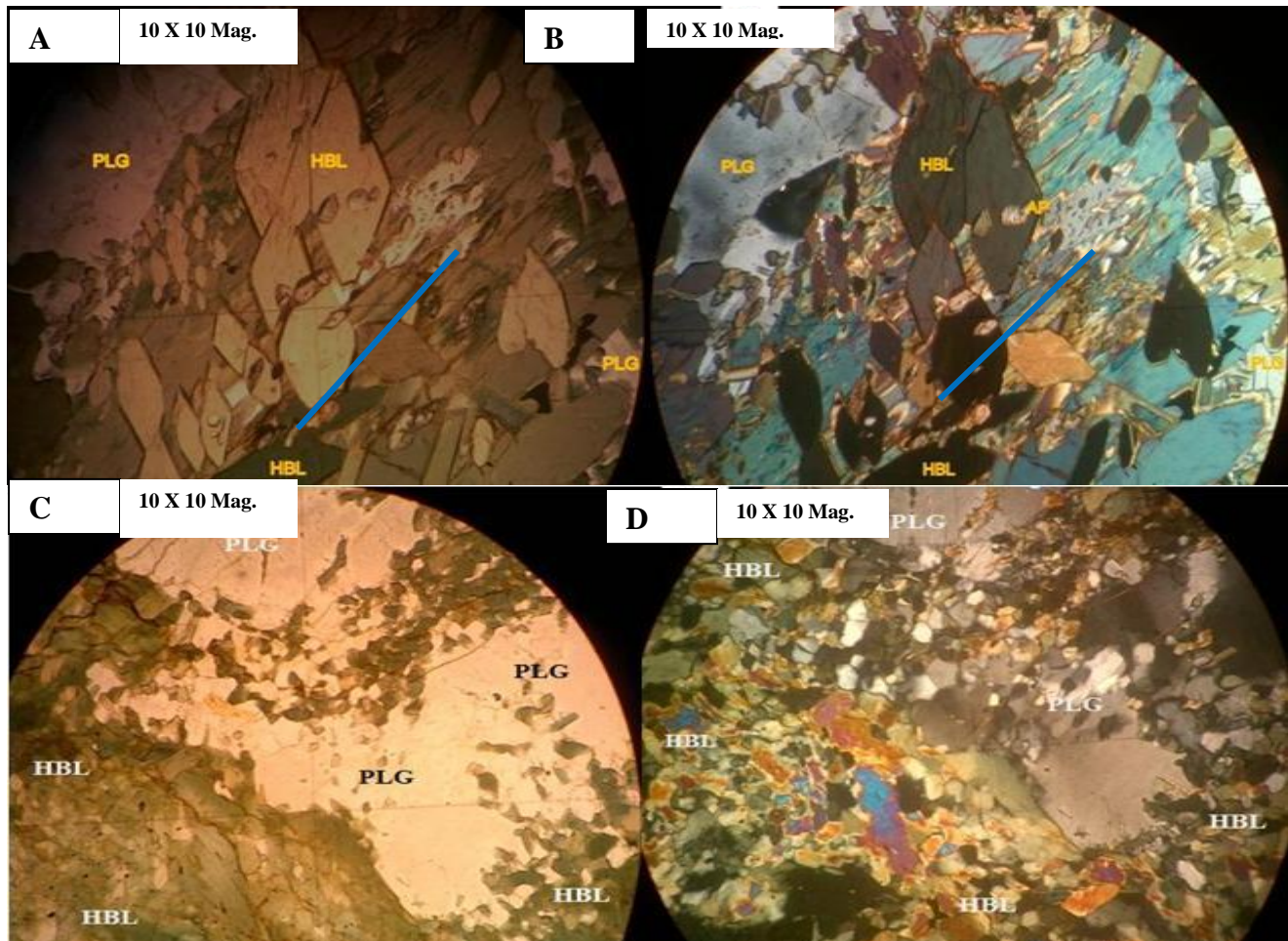


Figure.15. Photomicrographs (A&B) shows the schistose alignment of hornblende grains in direction along the line in hornblendite gabbro. (C&D) plane and crossed polarized light view of plagioclase and hornblende association in which hornblende exhibits the greenish to brownish color with an octahedral shape sometimes show grain alignments along a specific direction and it also shows fragmented grain appearance at the lower right of the section.

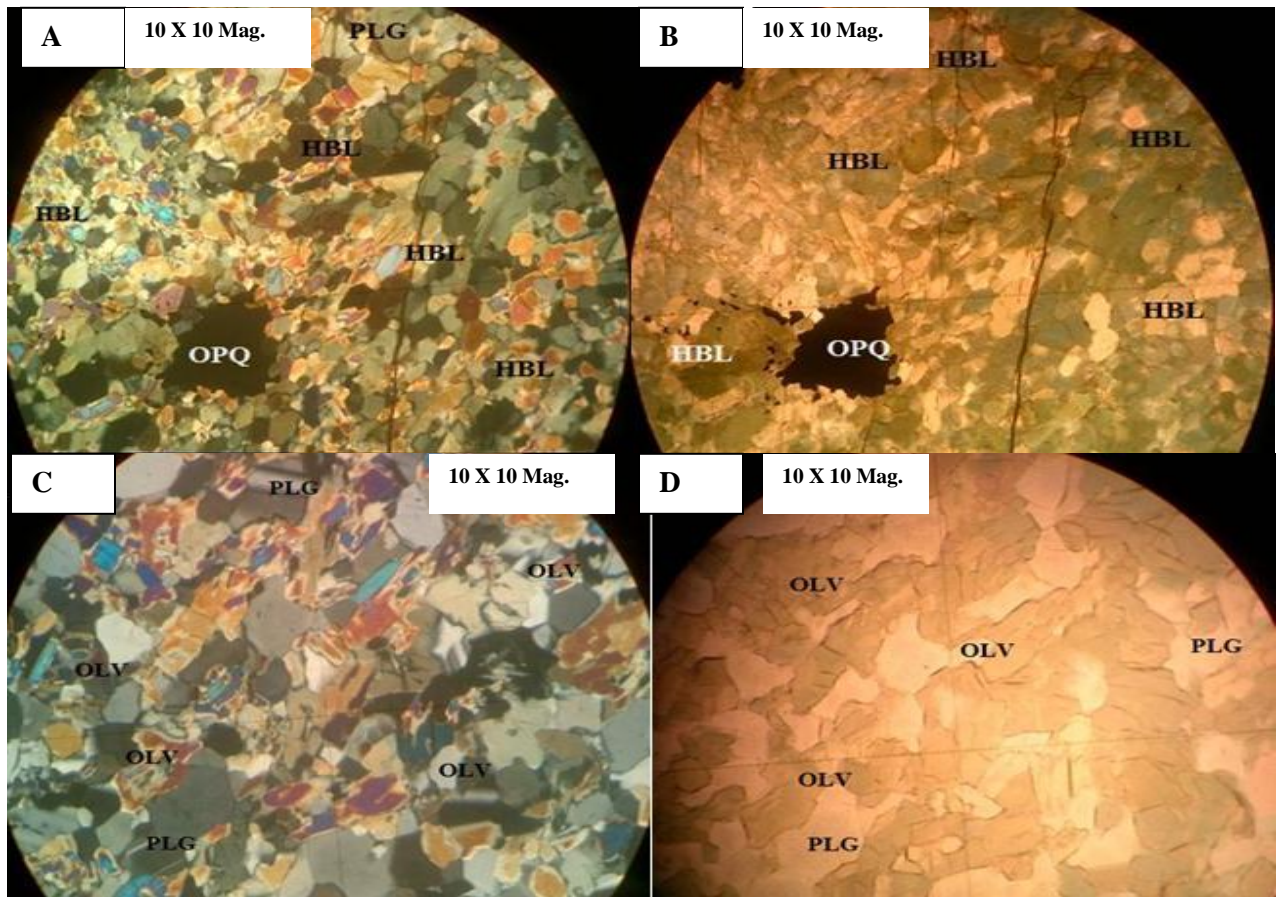


Figure.16. Photomicrographs showing (C) olivine (OLV), plagioclase (PLG) and hornblende (HBL) association with in the olivine gabbro is under crossed polarized light (D) is olivine gabbro under plane polarized light. (A&B) shows the crossed and plane polarized view of hornblende gabbro composed hornblende, plagioclase and opaque minerals.

4.7. FIELD AND PETROGRAPHIC RESULTS

Sample number	Sample code	Sample location	Description			
			Hand Specimen Description	Petrography Result		Rock Name
				Phase and Composition (%)	Thin Section Description	
1	DIT1S1	36816911 E 1029896 N	Black- gray, medium to coarse grained, and black and flakey grains of amphibole minerals are dominant	Olivine (30) Plagioclase (35) Hornblende (10-12) Opaque (7%) Biotite (Trace) Pyroxene (Trace)	Olivine is subhedral to anhedral with size ranges from 2- 5 mm. it is randomly distributed sometimes found in the plagioclase feldspar as a xenoblast texture. Plagioclase is subhedral to anhedral, very elongated sometimes rounded in shape with size ranges from 1.5- 6 mm. Opaque minerals are found in the olivine as xenoblastic texture with size ranges from 0.5- 3 mm.	Olivine gabbro
2	DIT1S2	36817646E 1030819N	Coarse grained hornblende containing rocks with other amphibole minerals which are rich in apatite			Olivine gabbro
3	DIT1S3	36817689E 1031096N	Coarse grained black-shiny minerals together with pinkish apatite are present.			Olivine gabbro

4	DITIS4 36817652 E 1031197N	Coarse grained with black shiny minerals with apatite minerals			Olivine gabbro
5	DITIS5 36817685E 1031478 N	Gray to brownish mica minerals present and they are coarse grained texture			Hornblende gabbro
6	DITIS6 36817718E 1031617 N	Variegated in color and coarse grained in texture with less amount of iron minerals with apatite.			Hornblende gabbro
7	DITIS8 36817182 E 1031753N	Exposed in the river cut	Hornblende (75-80) Plagioclase (12-15) Opaque (5- 8 %)	Hornblende minerals are dominant phase in this section with a grain size ranges from 1.5- 4.5mm. Opaque mineral grains are found as a xenoblast in hornblende and sometimes occur adjacent to it, the twin lamellae of plagioclase show a rounded boundry because of the deformation.	Hornblende gabbro
8	DITIS9 36816915E 103206IN	Apatite rich hornblende gabbro			

9	D2T2S1 36818525E 1031806N		Hornblende (60-65) Plagioclase (16-18) Quartz (5)	Anhedral crystal of hornblende grains show schistose alignment and have 2-4 mm size range. Plagioclase has elongated shape of size ranges from 2.5 – 5 mm and the twin lamellae are curved due to deformation.	Hornblende gabbro
10	D2T2S2 36818525E 1031806N	Composed of coarse grained and grayish color with flakey minerals.	Plagioclase(60) Hornblende (25) Apatite (5) Quartz (2) Opaque (6) Calcite (2) Biotite (<1)	Prismatic grains of hornblende show schistosity. Plagioclase grains have curved twin lamella. Some plagioclase contains inclusions of calcite. Prismatic grains of hornblendes are clustered together. Most of the apatites are enclosed in prismatic grains of hornblende.	Anorthosite gabbro
11	D2T2S3 36818249E 1031338N	It has high iron concentration.			Hornblende gabbro
12	D2T2S4-				Hornblende gabbro
13	D2T2S8 36818272E 1032180N	Variegated in color black, pink, and golden color mineral present. There is also presence of flakey minerals. Fine-medium grained texture.	Hornblende (63) Apatite (8) Opaque (10) Sphene (6) Plagioclase (9)	Schistose texture, prismatic grains of hornblende show sub-parallel to parallel orientation. Prismatic and hexagonal grains of apatite are enclosed in hornblende aggregates. Very fine opaque minerals are grown in the hornblende matrix.	Hornblende gabbro

14	D3T1S1 36812538E 1025396N	Iron containing sample.			Hornblende gabbro
15	D3T1S2 36817984E 1030536N	Iron zone boundary above which the apatite bearing zone is overlies S-N trending structure	Hornblende (80) Apatite (10) Opaque (10)	Hornblende aggregates are randomly distributed over the groundmass. Prismatic and subrounded grains of apatite are also occurring over hornblende groundmass. Some apatite grains also enclosed in opaque minerals.	Hornblende gabbro
	D3T1S3 36818140E 1030250N	The iron is hosted by the olivine rich gabbro			Olivine gabbro
16	D3T1S4 36818131E 1030257N		Hornblende (38) Biotite (8) Quartz (18) Plagioclase (25) Opaque (8) Apatite (3)	Biotite flakes and prismatic grains of hornblende show well developed schistosity. Some hornblendes are replaced by biotite. Apatites are enclosed in hornblende (rounded-sub rounded).	Hornblende gabbro
17	D3T1S5 36818108E 1030295N				Hornblende gabbro
18	D3T1S6 36818163E 1030169N	There is fault trending NW-SE			Hornblende gabbro
	D3T1S7 36818108E 1030295N		Hornblende (57) Apatite (18) Opaque (14) Biotite (11)	Schistose and prismatic grains of hornblende and biotite show preferred orientation. Apatite grains are bounding the opaque minerals and others are enclosed.	

19	D4T1S7 36818156E 1030148N	Gabbro which is olivine deficient	Hornblende (54) Plagioclase (15) Calcite (2) Opaque(17) Biotite (2) Apatite (10)	Apatite is found in hornblende. Plagioclases are elongated and contain inclusions of calcite. Granules of opaque minerals are found in hornblende. Some apatites are seen at the boundaries of opaque grains.	Hornblende gabbro
20	D3T1S8 Trench Three 36818212E 1029840N	Occur near to the stream which is at the downslope. The iron is very concentrated and when it goes up the iron content reduced and the apatite becomes mixed with the iron. Therefore the trench shows that the iron content increases downward.	Hornblende (53) Plagioclase (<26) Opaque (<10) Sphene (<6) Apatite (<4) Biotite (<1) Chlorite (Trace)	The matrix composed of hornblende and plagioclase is showing parallel to subparallel alignment definitely schistosity and opaque minerals are rimmed by sphene. Plagioclase lost its twin lamellae due to deformation.	Hornblende gabbro

Table.1. Field and petrographic description of different rock samples such as: olivine gabbro, hornblende gabbro, hornblendite gabbro, and anorthosite gabbro.

4.8. GEOLOGICAL STRUCTURES

In Bikilal intrusive iron ore body, different structural phenomena such as: foliation, schistosity shearing and faults are observed. Generally the faults are subdivided into NNW-SEE and NE- SW systems. The NWW- SEE fault is cut by NW –SE fault which in turn is cut by NE- SW fault. Faults don't show pronounced displacement except fracturing of the rocks. The rocks in faults zones are altered to fractured breccia and to cataclastic. Width of the fault zone ranges from tens of centimeters to some meters. The strike length ranges from some meters rarely up to a few kilometers. The dip of the faults ranges from 35° to 75° .

Fault structures which are Post to mafic- ultramafic intrusion observed around the iron ore deposit. Individual fractured shear zone have a restricted strike extension. Influence of fracturing and shearing are seen on the ore bodies. Furthermore, fractural fissures of ore body occurs filled by stringers of sulphide injections.

Generally all geologic units in the area are dipping towards the center of the intrusive and major structural trends are reflected in the regional lineaments of the study area trending NW – SE and NE – SW.

4.9. DRILLHOLE DATA LOGGING IN BIKILAL INTRUSIVE BODY

Borehole data are used to prepare different log sections and their lithological correlation with each other. The data was collected from Geological Survey of Ethiopia and the drilling works were done by the Consult 4 International in 1996 in cooperation with geological survey of Ethiopia for phosphate exploration work. Even though this drilling project was conducted for the apatite exploration, it is also help full to understand the subsurface geology of the study area and to infer the depth at which iron mineralization could be possibly inspected because the drilling work was within the same area.

4.9.1. DRILLHOLE LOG CORRELATION

Based on the borehole data found from the Geological Survey of Ethiopia it is possible to formulate different log sections and correlate them according to their lithological similarity. Different lithology in the log sections are represented by different colors and letters.

As it is evidenced by the log sections below, different gabbroic units show layering. The thickness of the gabbroic intrusive layering is not the same for all logs in the area rather it display range of thickness even in single drill hole. The thickness of A- type lithology in the log ranges from few cm upto hundreds of meters. And type- B lithology shows a thickness range from few cm to 35-40 meters. A and B – type lithology are the most dominant rocks in most of the log sections.

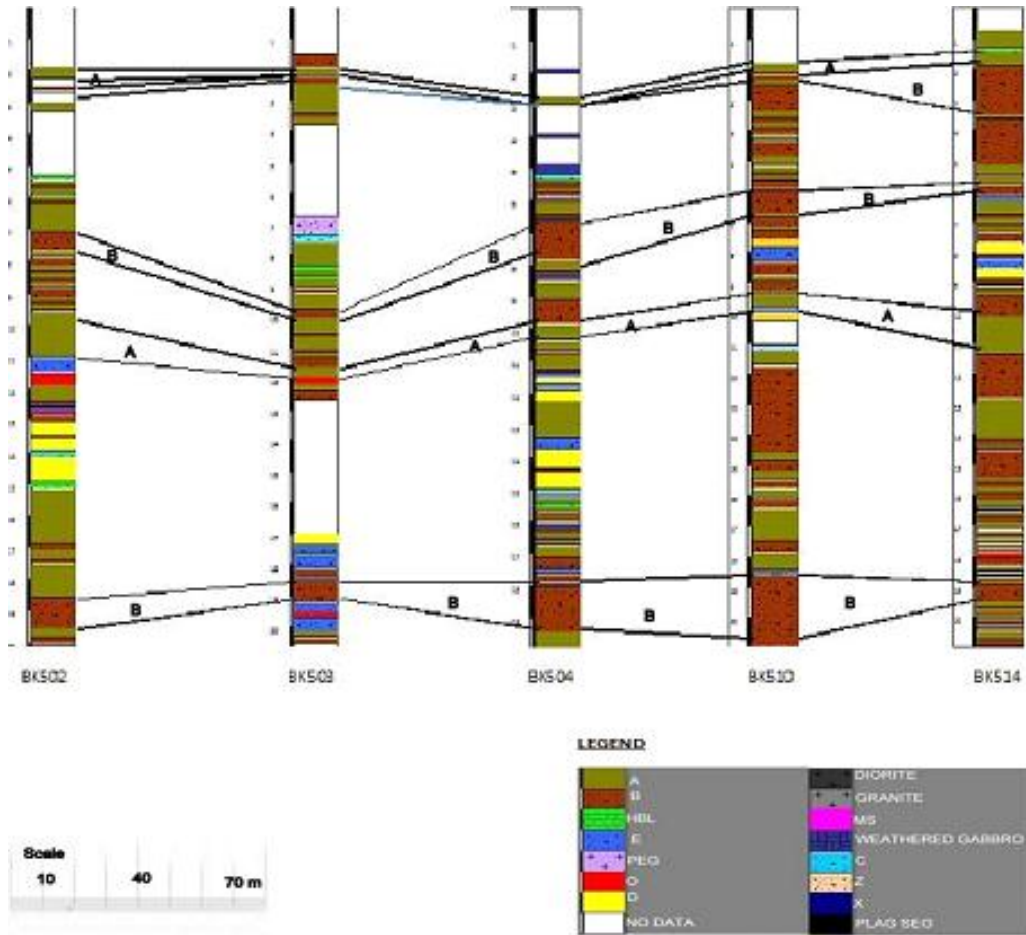


Figure.17 (A) Correlation of different borehole loges; Amphibolite gabbro (type A) which has melanocratic to leucocratic color and at the depth below 53m these unites bear ilmenite and apatite, olivine gabbro (type B) this letter stands for intercalation of type-A and E, hornblendites (HBT) are the ilmenite bearing hornblendite gabbro zones in almost all boreholes. Sulfide minerals are found within the amphibole gabbro type (A, E, X, and Z), hornblendite, and olivine gabbro (type B). Apatite is reach in the amphibole gabbro (type A), hornblendite (HBT), and amphibole gabbro (type D). C stands for anorthosite gabbro, D stands for amphibolite gabbro showing banding of mafic and felsic zones and perpendicular to the banding veinlet of quartz, and chlorite, present, E represents amphibolite gabbro intercalation with olivine gabbro some sulphide minerals are also present, PEG is a symbol for a pegmatite intrusion, letter O stands for amphibolite gabbro, letter X stands for amphibolite gabbro with purple phenocrists, letter Z represent chloritized amphibolite gabbro, MS stands for meta-sediments, Plag Seg is a symbol of plagioclase segment After Consult 4 International (1996)

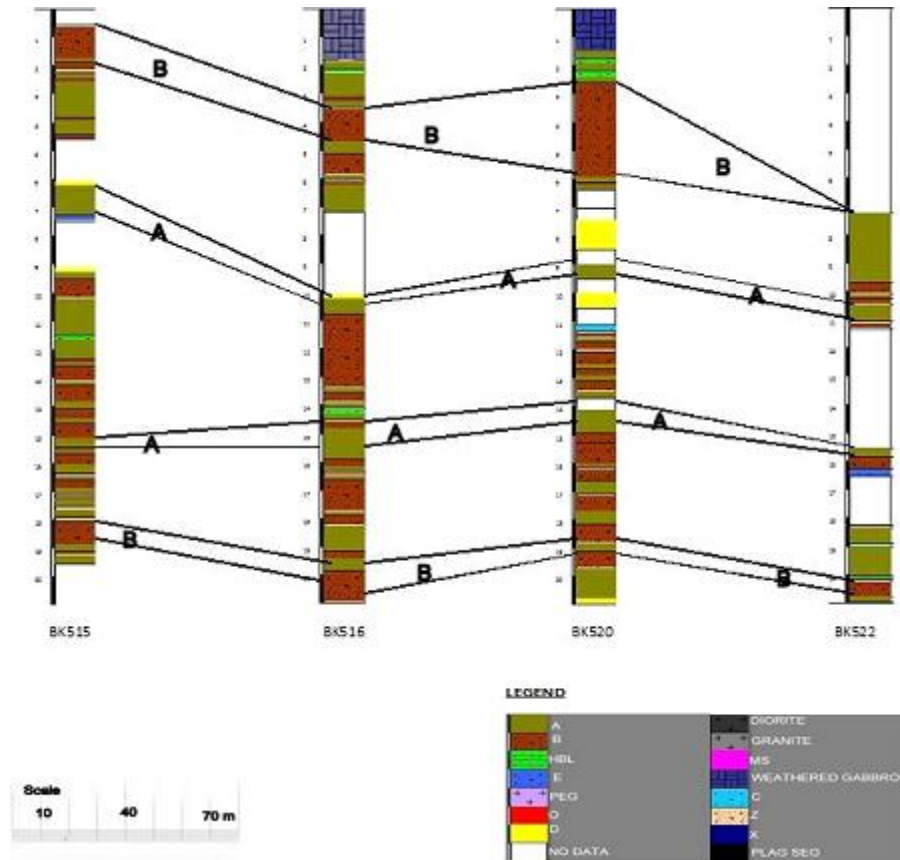


Figure.17 (B) Correlation of different borehole logs; Ilmenite and magnetite are found in the amphibole gabbro type (A, E, & X) and in the hornblendite zones. Apatite is dominantly found in amphibole gabbro (type A, E), HBT, and in small amount in olivine gabbro (type B), zones. Sulfides are found at different intercepts of amphibolite gabbro type (A, D, and E) and rare in olivine gabbro (type B) and amphibolite gabbro (type Z). After Consult 4 International (1996)

5.1. MINERALIZATION

Ultramafic rocks are the host for several metallic and industrial minerals including chromite, Fe, Ni, Cu sulphides, and PGM (Scott et al. 2000). Magnetite- ilmenite ore bodies in Bikilal deposit are genetically and spatially related with basic-ultra basic gabbroic intrusive rocks. Ore bodies are distributed with in the area where hornblendite are mixed and alternated with anorthosite and hornblende gabbro. Hence the ore bodies are mostly localized within the hornblendite gabbro and rarely in its vicinity. Hornblendite gabbro belt consists of irregular lens and is composed of hornblende, plagioclase and amphibole forming linear shape of parallel layers and sometimes showing laminated layers. The hornblendite belt is 1- 1.2 km wide and is more than 15 km long (Ethio-Korean iron exploration project, 1988).

According to Ethio-Korea iron exploration project (1988) iron ore bearing hornblendites are classified into three zones:

1. Upper zone in the northern part,
2. Middle zone in the north- eastern part,
3. Lower zone in southern part

In general, the strike and dip of the ore bodies follow the trend of hornblendite. The upper zone runs NW- SE and dips to south at angle of 70° - 80° . The middle zone strikes NW-SE and N-S and dip to west at angle of 70° - 85° and occasionally to east at angle of 70° - 85° . The lower zone strikes NE-SW and N-S and dip to northwest at an angle 60° - 85° occasionally to S-E at an angle of 70° - 75° .

The iron ore bodies are generally occur as a massive or disseminated type. The massive and disseminated ore minerals occur within hornblendite gabbro and rarely in hornblende gabbro.

Barren hornblendite and rocks composed of plagioclase and amphibole are sandwiched with in ore bodies. Sizes of the ore bodies exposed on surface vary in strike length from 60-250

meter and in width from 4-6 meter to 30-40 meter wide. Total length of iron ore- bearing zones is 4900 meters and length of ore bearing zones being 700 meters (Ethio-Korea, 1988).

Bikilal iron ore deposit consists of minerals like magnetite, ilmenite, hematite, sulphides, apatite and gold. From these the principal ore minerals are magnetite and ilmenite. Based on the ore microscopic studies, the ore mineral assemblages consists of 5-12% ilmenite, 20-25% of magnetite, >10% of hematite, and small amount of sulfides (pyrite, pyrrhotite, and chalcopyrite, pentlandite) in average. In this ore body hematization and meritization of both magnetite and ilmenite is very common.

The main gangue minerals are quartz, K-feldspar, biotite and chlorite while calcite, sphene, rutile, and goethite are minor gangue minerals.

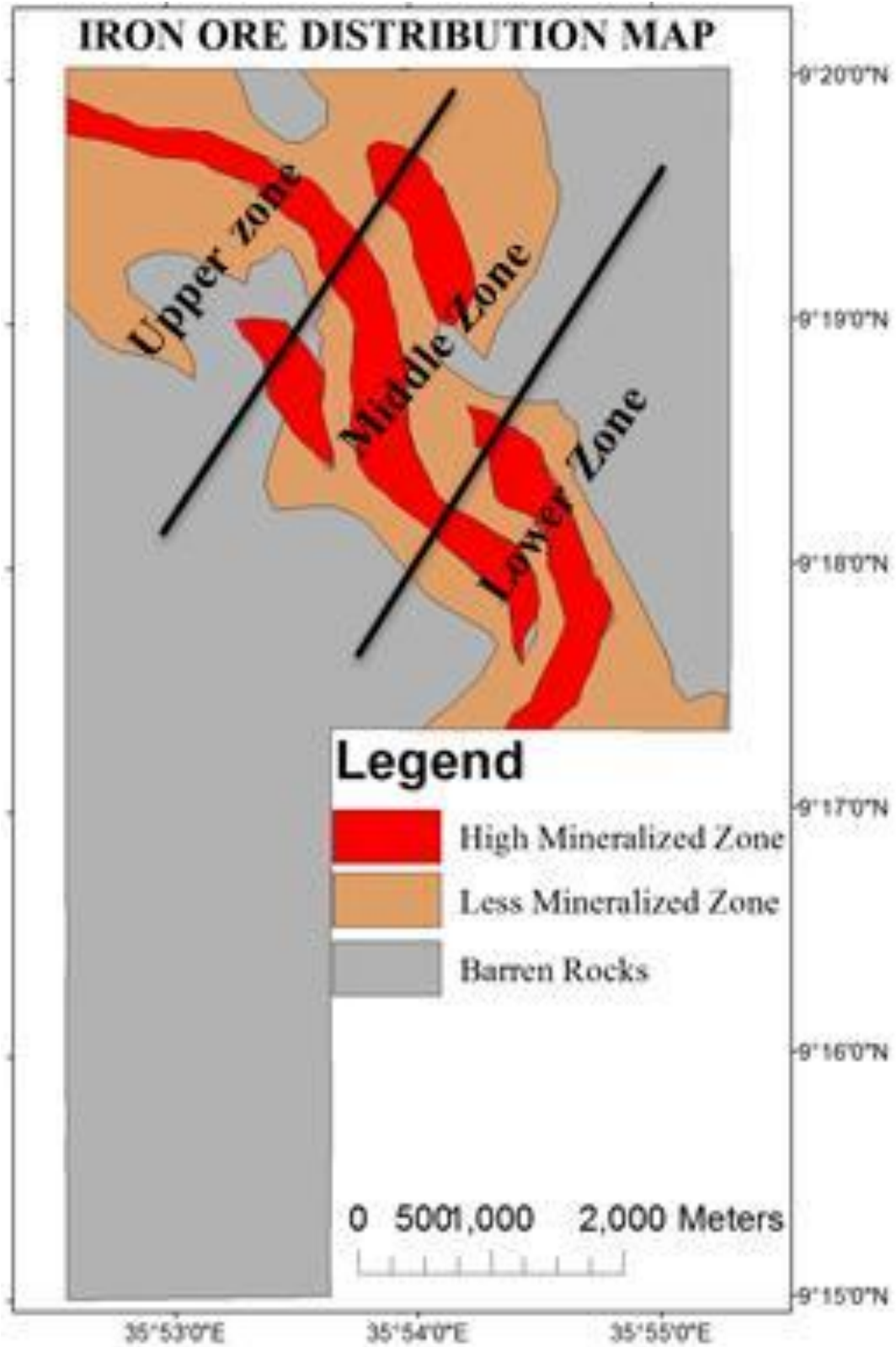


Figure.18. Map showing iron ore distribution in Bikilal iron ore deposit.

5.2. ORE MINERALS

Ten representative samples were selected for polished section analysis. During these analysis works the following ore minerals were identified: magnetite, ilmenite, hematite, goethite, hydro-goethite, pyrrhotite, pyrite, chalcopyrite, pentlandite and gold. The results of this laboratory work are presented below in tabular form.

Sample code	Mineral Composition	Percent age (%)	Description of the Specimen
D2T1S8	Magnetite	30- 35	Magnetite occurs as a ground mass and it appear as a relict, poikilitic sometimes as veinlet and it is exsolved into lamellar ilmenite (Fig.20 (E)). Ilmenite is pink to pinkish brown showing slight pleochroism and it is replaced by crosshatched texture of hematite (Fig.19 (B)). Later hematite is transformed into goethite especially at the periphery or grain boundary(Fig.19 (B))
	Ilmenite	5-10	
	Geothite	12-15	
	Gangue	25-30	
	Pyrite	Trace	
	Hematite	5-10	
D3T1S10	Ilmenite	10-12	Ilmenite occurs as a veinlet following the gangue minerals (Fig.19 (A), 21(C), 22 (A)) and sometimes they appear as a poikilitic grain. Some grains of ilmenites are replaced by goethite. Pyrites is light yellow, anhedral to cubic shape occur as a poikilitic along with veinlet ilmenite. Goethite is brown to deep brown found as a replacing texture of pyrite and ilmenite.
	Gangue	85	
	Pyrite	2-3	
	Geothite	2	
D3T1S5a	Magnetite	10-15	Magnetites occur as a veinlet following the gangue minerals, sometimes as a poikilitic (Fig.19 (C&D), 21 (B&D)) and 22 (B).It is replaced by hematite and later the hematite is replaced by goethite. Pyrite is irregular in shape and grows inside the gangue minerals as
	Hematite	3	
	Pyrite	4-5	
	Geothite	2	
	Gangue	70	

			inclusion (Fig. 22 (D)), sometimes grows along with magnetite (Fig.19 (D), 21 (A), &22 (B)). It is small in size (1mm- 3mm). Like magnetites pyrite grows as a veinlet following the gangue mineral and later it is replaced by goethite at the grain boundary (Fig.22 (A)).
D2T2S8	Pyrrhotite	10-12	Pyrrhotite is creamy white occur as a veinlet following the gangue minerals and show irregular shape (Fig. 22 (C)). It is also occur as inclusion in pentlandite (Fig.22 (A)). Some grains of it replaced by chalcopyrite. Magnetites develop inside the gangue as a veinlet following the gangue minerals and have a lath shaped grains. Gold grains are also found as patched minute grains inside the chalcopyrite of yellow color with a greenish tint. Pyrite occurs as anhedral inclusion in the gangue mineral phase (Fig.19 (D), 22 (D)). Some grains of pyrite are replaced by chalcopyrite. Chalcopyrite is deep yellow occur as inclusion in the gangue and grows along with magnetite as a poikilitic grain (Fig.21 (C&D), 22 (B)). It also encloses gold grains as inclusion (Fig.23 (B)).
	Chalcopyrite	3	
	Pyrite	5-6	
	Magnetite	2-3	
	Gold	1	
	Gangue	77	
D3T1S4	Ilmenite	25-30	Ilmenite occurs as a veinlet following the gangue minerals and later replacement by hematite is very common. Inclusion of pyrite is present inside the ilmenite and in gangue minerals. Some grains of pyrite are replaced by goethite at grain boundary. Geothite occur as a replacing of hematite and later replaced by hydro-goethite Fig.20 (A) & 21 (A &C)).
	Hematite	10-15	
	Pyrite	1	
	Geothite	3-5	
	Hydro-goethite	2	
	Gangue	47	
D3T1S5 b	Magnetite	10-15	Magnetites occur as a veinlet following the gangue minerals, sometimes as a poikilitic. It is replaced by
	Pyrite	2	

	Goethite	3-5	hematite and later the hematite is replaced by goethite. Pyrite is irregular in shape and grows inside the gangue minerals as inclusion, sometimes grows along with magnetite. It is small in size (1mm- 3mm). Like magnetites pyrite grows as a veinlet following the gangue mineral and later it is replaced by goethite at the grain boundary (Fig 21 (A), 22 (B)).
	Gangue	79	
D3T1S9 b	Ilmenite	15	Ilmenite occurs as a veinlet following the gangue minerals. Pyrite is disseminated as inclusion on the gangue minerals and minor inclusion of it is replaced by hematite. Free grains of gold occur as inclusion in the gangue mineral in association with pyrite (Fig.23 (A)).
	Pyrite	4	
	Hematite	1	
	Gangue	80	
	Gold	1	
D3T1S9 a	Ilmenite	15	Ilmenite occurs as a veinlet following the gangue minerals. Pyrite is disseminated as inclusion on the gangue minerals and minor inclusion of it is replaced by hematite.
	Pyrite	4	
	Hematite	1	
	Gangue	80	
D3T1S8 G	Ilmenite	18	Ilmenite occurs as a veinlet following the gangue mineral. Pyrite occurs as inclusion in the gangue minerals.
	Pyrite	5	
	Gangue	77	
D2T2S4	Ilmenite	46	Ilmenite occurs as a poikilitic texture. Major irregular mass of ilmenite is replaced by platy hematite. The ilmenite is strongly hematized (Fig. 20 (A, C, D& E)).
	Hematite	26	
	Goethite	6	
	Hydro- goethite	2	
	Gangue	20	

Table.2. Ore microscopic result

5.3. DESCRIPTION OF ORE MINERALS

5.3.1. MAGNETITE

Magnetite is one of the dominant iron ore mineral generally observed in Bikilal iron ore deposit. Magnetites occur as a well-developed crystal, but commonly filling the interstices as a veinlet following silicate minerals. Magnetite grains have subhedral to anhedral shape with grain size ranges from 0.1 - 1.5 mm occasionally exceeds 1.5 mm in some sections. Sometimes magnetite occurs as cumulus irregular grain with commonly relict, poikilitic or as a veinlet texture following the gangue minerals and in some sections it occurs adjacent to ilmenite crystals (Fig.19.C). Coarse grained magnetite crystals grow in the silicate phase which may indicate minerals were crystallized at high temperature of early differentiated stage (Fig.21.B). Magnetites are found as ground mass in some sections, in which lamellar exsolution feature of ilmenite is replacing over it and this type of replacement can be refer as ilmeno-magnetite (Fig.19.A&Fig.20.E). Ilmeno- magnetite is later transformed in to hematite and goethite (Fig.19.A & B).

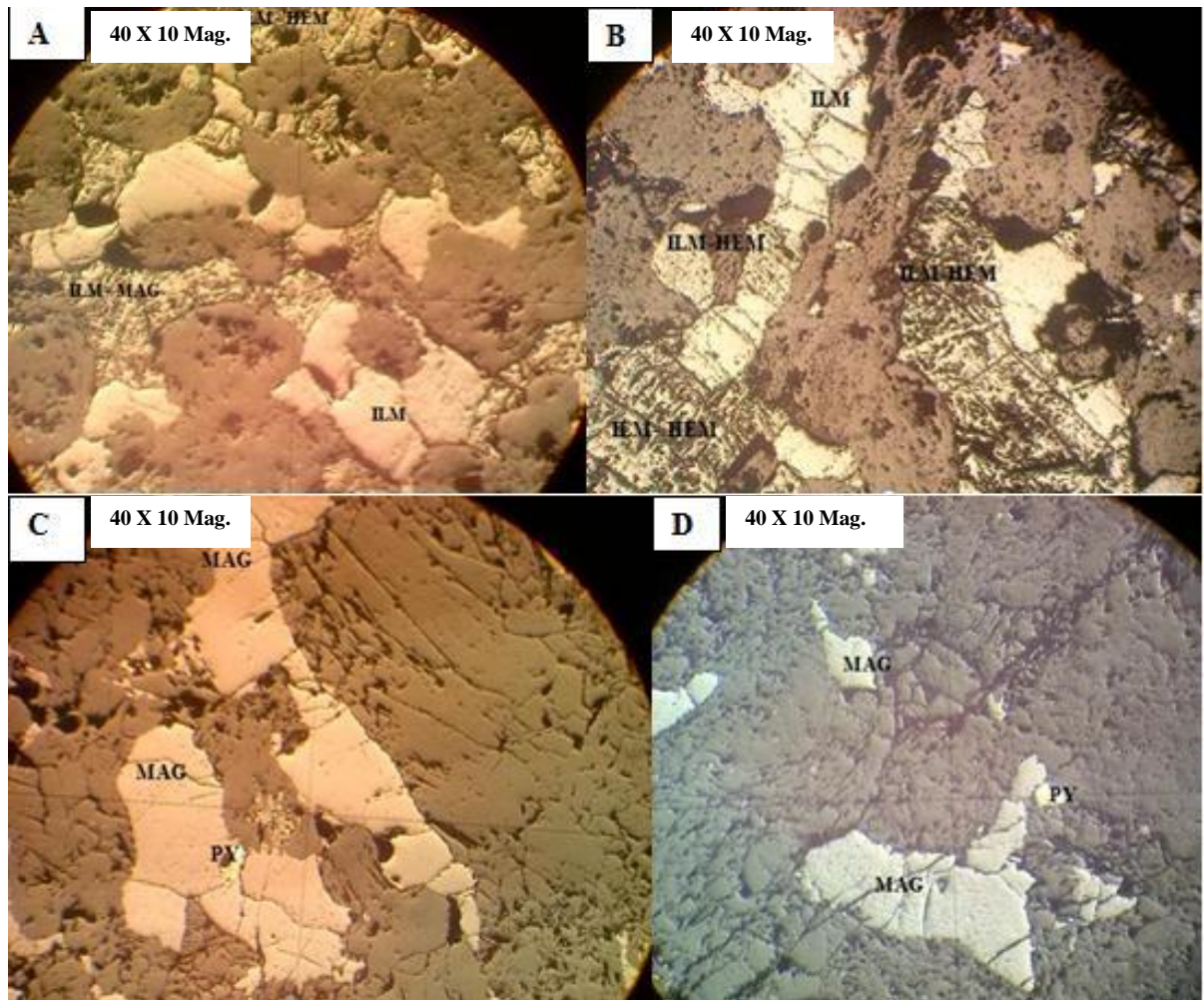


Figure. 19. Photomicrographs of magnetite, pyrite and oxidation textures of ilmenite A) Exsolution lamellae of ilmenite in magnetite oxidation (stage III) B) Hematite replacement of ilmenite (stage III) C&D) adjacent growth of veinlet magnetite with pyrite (stages II).

5.3.2. ILMENITE

Ilmenites are the second dominant iron ore minerals generally observed in Bikilal iron ore deposit. Ilmenites occur as a veinlet following the gangue minerals and as an exsolved lamellar texture in magnetite (Fig.19.A&Fig.20.E). Some grains of ilmenites are replaced by hematite then by goethite and some occur as elongated exsolution textures in magnetite (ilmeno-magnetite) (Fig.20.D). Exsolution lamellae of ilmenite in magnetite range from few μm to mm in thickness and reach up to several μm in length (Fig.20.E). However, some ilmenite grains contain fine particles of hematite and isolated rows of hematite having their long dimensions parallel to each other. Commonly, the dust like particles are evenly distributed throughout the ilmenite grains, though the abundance of exsolution varies from grain to grain. Coarse-granular ilmenite consists of a variety of hematite as exsolution and replacement textures are very common (Fig.20.D).

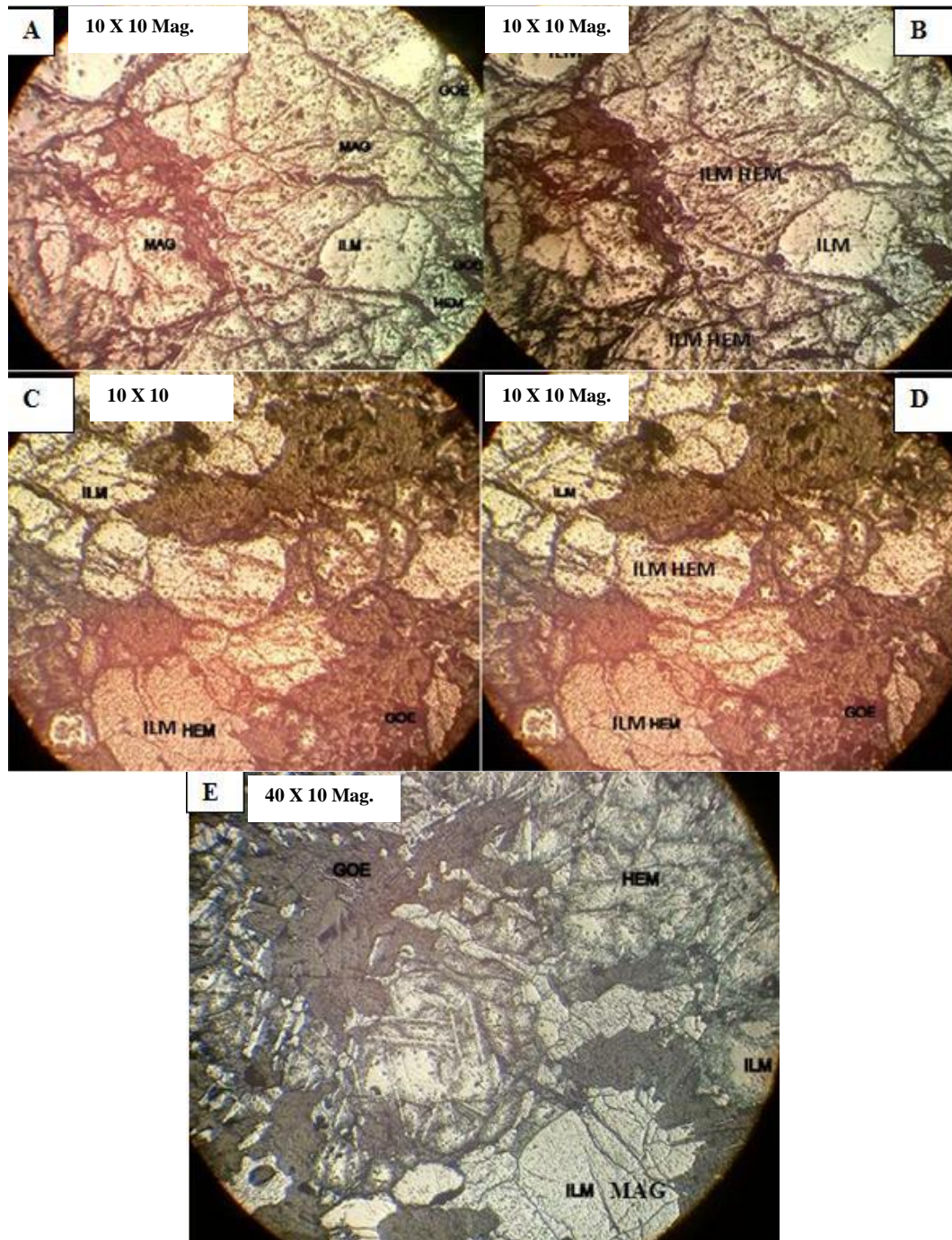


Figure.20. Photomicrographs of oxidation textures of magnetite and ilmenite A) Total exsolution replacement of groundmass magnetite (MAG) by ilmenite (ILM) (stage III) B) Hematite(HEM) replacement in ilmenite (ilmeno-hematite) (stage III-III) C) Increasing intense oxidation and hydration will replace ilmenite as host by hematite and goethite (stages III-IV) D) Ilmenite with hematite replacement as a sieve texture (stage III-IV). (E)Exsolution of ilmenite from magnetite.

5.3.3. HEMATITE

Hematite is an altered oxidation product of magnetite and ilmenite. Hematites occur as crosshatched replacing texture of ilmenite especially at the grain boundary while some occur as replacing texture of magnetite later replaced by goethite in both cases (Fig.20.A). In some sections hematite occur due to alteration of pyrite at the grain boundary.

5.3.4. GEOTHITE AND HYDRO- GEOTHITE

Goethite and hydro-goethite are secondary minerals occur as a replacing texture in hematite, pyrhhotite, pyrite and chalcopyrite minerals due to reaction with water. Latter goethite is transformed into hydro-goethite as the intensity and duration of water and other iron containing ore minerals interaction increases.

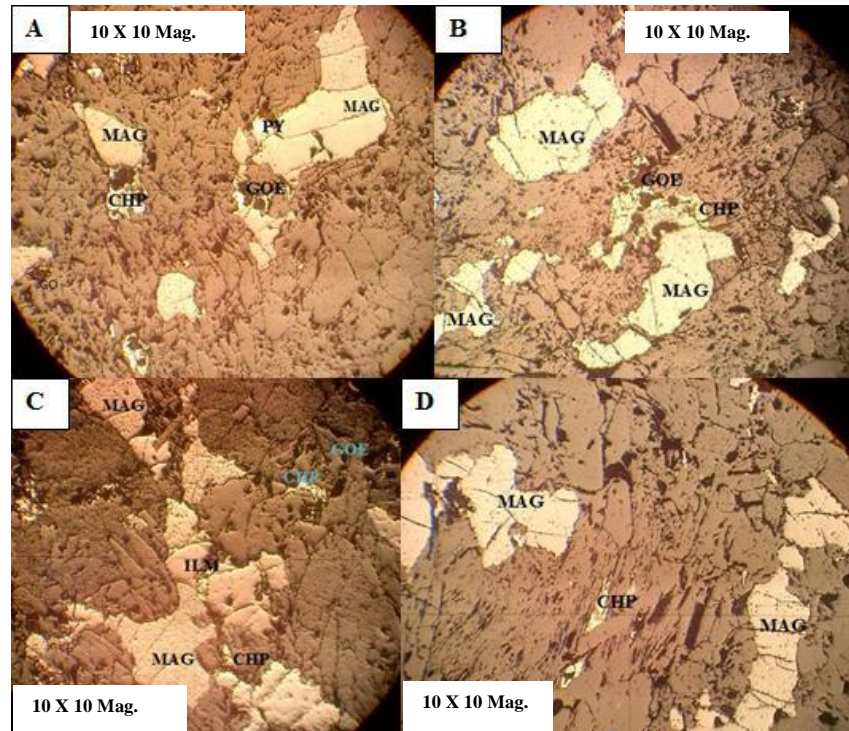


Figure.21. Photomicrographs association of magnetite, pyrite, chalcopyrite and goethite A) Poikilitic and veinlet magnetite (MAG) grains adjacent to chalcopyrite (CHP) later the chalcopyrite replaced by goethite (GEO) (stage II-III) B) goethite replaces the chalcopyrite (stage IV) C) magnetite and

ilmenite (ILM), and chalcopyrite grows within the gangue and later CHP replaced by the goethite D) magnetite and pyrite (Py) grows within the gangue.

5.3.5. PYRRHOTITE

Pyrrhotite have a creamy white and occur as disseminated patches in gangue mineral (Fig.22.C) or as large anhedral grains commonly enclose in pentlandite associated by minute magnetite octahedral grains (Fig.22.A). Sometimes Pyrrhotite grains are partly or completely replaced by chalcopyrite and goethite along grain boundaries. Pyrrhotite is also grows as a veinlet following the gangue minerals and some grains of it replaced by chalcopyrite.

5.3.6. CHALCOPYRITE

Chalcopyrite encloses minute grains of goethite as replacing texture, usually adjacent to ilmimo-magnetite (Fig.21.A). They are deep yellow in color and anhedral to subhedral in shape. Some chalcopyrite grains enclose minute grains of gold which have yellow color with greenish tint as inclusion (Fig.23.B). Chalcopyrites are also occurring as replacing texture of pyrite and pyrrhotite along the periphery (Fig.22.A). Chalcopyrite and pyrite are the common sulfide phases; usually occur as minute inclusions in the silicates or as composite grains mostly cracked and altered to goethite.

5.3.7. PYRITE

Pyrite is light yellow in color, anhedral to cubic shape with high reflectance than chalcopyrite and occurs as poikilitic texture in the gangue mineral (Fig.19. D). These minerals are small in size 1mm- 3mm. Pyrite, like magnetites grows as veinlet following the gangue minerals (Fig.22.A) Some grains of pyrite also occur as inclusion in ilmenite and sometimes pyrite occur as disseminated inclusion in gangue minerals and minor inclusion of it is replaced by hematite and goethite (Fig.22.B).

5.3.8. PENTLANDITE

Pentlandite is light gray usually present in gangue minerals with sharp and irregular margins adjacent to pyrite and ilmenite (Fig. 22 (A)).

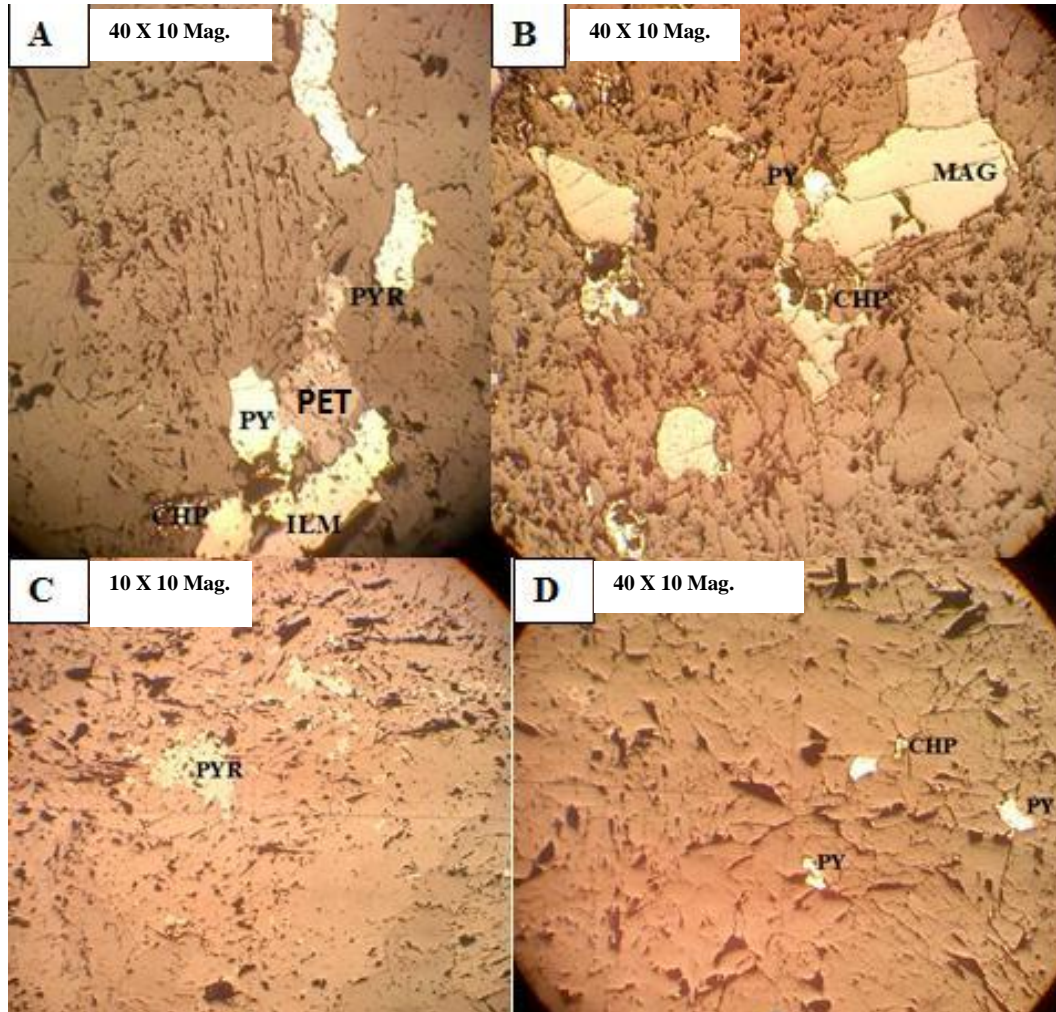


Figure.22. Photomicrographs showing magnetite (MAG), Pyrite (PY), Pyrrhotite (PYR), Pentlandite (PET), and Chalcopyrite (CHA). A) Pyrrhotite grows inside the pentlandite in association with pyrite and CHP B) magnetite grow adjacently to pyrite C) association of chalcopyrite and pyrite with in the gangue mineral D) pyrrhotite in the gangue mineral.

5.3.9. GOLD

Gold minerals occur in association with sulphide minerals like pyrite, chalcopyrite, pentlandite and other gold pathfinder minerals; generally it has an affinity with chalcophile elements. Basically in Bikilal magnetite- ilmenite ore deposit, occurrence of pyrite, chalcopyrite, pyrrhotite, pentlandite and Au association is very common. Gold grains are found as isolated grains in association with other sulphide minerals but commonly it occur as hatched inclusion in chalcopyrite (Fig.23 (B)). Under microscope it resembles chalcopyrite in color but the main difference between them is; gold has a greenish tint while rotating the stage of microscope. This is classic characteristics of gold mineral which is important to distinguish gold from other confusing sulphide minerals. Chalcopyrite unlike the gold doesn't display greenish tint during rotation of the microscope stage. Minuet gold grains are also identified in some sections as inclusion in the chalcopyrite (Fig.23 (A)).

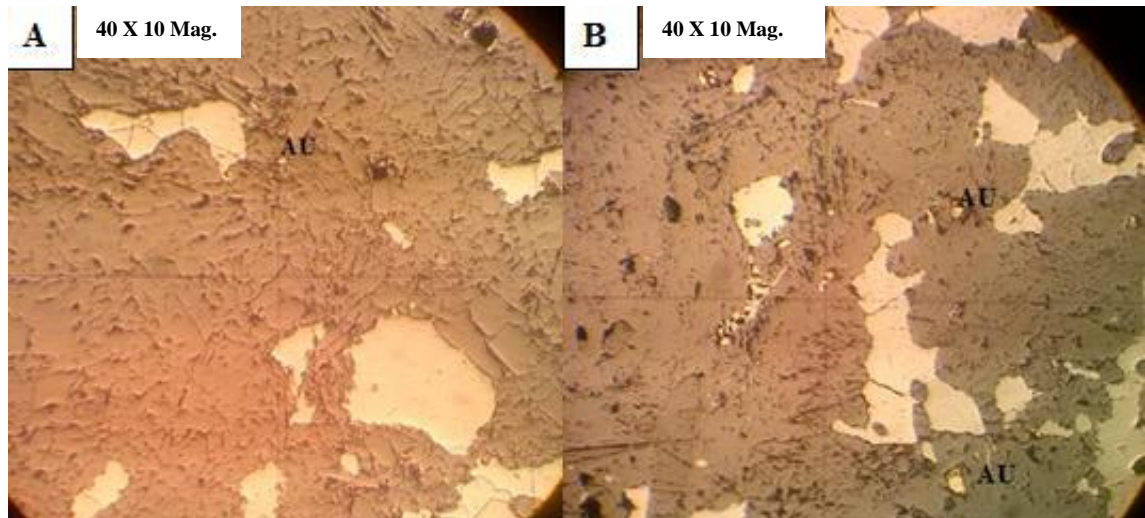


Figure.23. Photomicrographs showing Gold (AU) grains at Bikilal iron ore deposit. A) Free Gold grains B) Hatched Gold grains inside the chalcopyrite.

5.3.10. APATITE

Apatite is most abundant associated mineral in Bikilal magnetite- ilmenite ore deposit. Apatite occurs as rounded to sub- rounded sometimes as elongated prismatic crystals. Prismatic apatite occurs in association with the opaque minerals (with magnetite and ilmenite) and hornblende crystals (Fig.15 (B)). In hand specimen apatite appears as soapy pinkish in color. Some of the apatite minerals appear to have suffered from surface weathering. Under microscope, apatite is colorless and it is easily recognized by its high relief, low birefringence and absence of good cleavage. Generally based on the field and microscopic observation apatite found associated with iron ore in apatite bearing hornblende gabbro and hornblendite gabbro.

5.4. ALTERATION

The dominant ore minerals in Bikilal intrusive are mainly magnetite and ilmenite other than phosphates, but surficial ore contains more martite & hematite resulted from a process of martization and oxidation. The ore minerals found at depth are free of martite and limonite, because of the unavailability of the ore to weathering process.

Field observations, combined with gradational contact of the olivine gabbros seen in some places, suggest a metasomatism at late stage magmatism may have played a role in the formation of hornblende gabbro. Olivine gabbros are apparently fresh, but traces of metasomatism may be present. Generally hornblende gabbro found at the periphery of the intrusion is severely affected by chloritization, sericitization, oxidation, and tremolitization. The most common oxidation alterations are change of magnetite and ilmenite to hematite or limonite. Sulfide minerals often weather easily because they are susceptible to oxidation and replacement by other iron oxide minerals. In Bikilal iron ore deposit alteration of pyrite and chalcopyrite to pyrrhotite or goethite is very common.

5.5. PARAGENESIS

Fe-Ti oxide minerals reveal several paragenetic information about the rocks containing them and their micro textures providing important knowledge of the prevailing oxygen, pressure and temperature (Buddington and Lindsley, 1964). Magnetite shows intense oxidation assemblage of different paragenetic sequence, from homogeneous magnetite, exsolution lamellae of ilmenite to oxidation textures of hematite and goethite (Fig.20.A). The lamellae are concentrated in the center of the magnetite grains. When magnetite exposed to intense oxidation state, exhibits an alteration to hematite with a complete pseudomorphic replacement by ilmenite. Magnetite also shows an extensive martitization and oxidation replacement.

Due to the effect of oxidation magnetite have been changed into martite and hematite. According to drill hole data the ore minerals are very simple in Bikilal iron ore deposit, i.e. hematite or martite at the surface and magnetite at depth.

Hematite and ilmenite formed by oxidation of Ti-bearing magnetite during retrograde metamorphism and this is evidenced by the coexistent of metamorphic minerals like chlorite and calcite. Lamellar texture of exsolution ilmenite in the magnetite developed broadly in all magnetite exposed in the surface. Exsolution ilmenite is arranged as parallel plates and has a lattice shape. Very tiny plates of hematite are also arranged in lattice shape due to martitization.

Based on the integration of microscopic study (textural relationship, mineral assemblages and ore fabrics) with preexisting geochemical data, four sequences of mineralization phase are recognized (Fig.24).

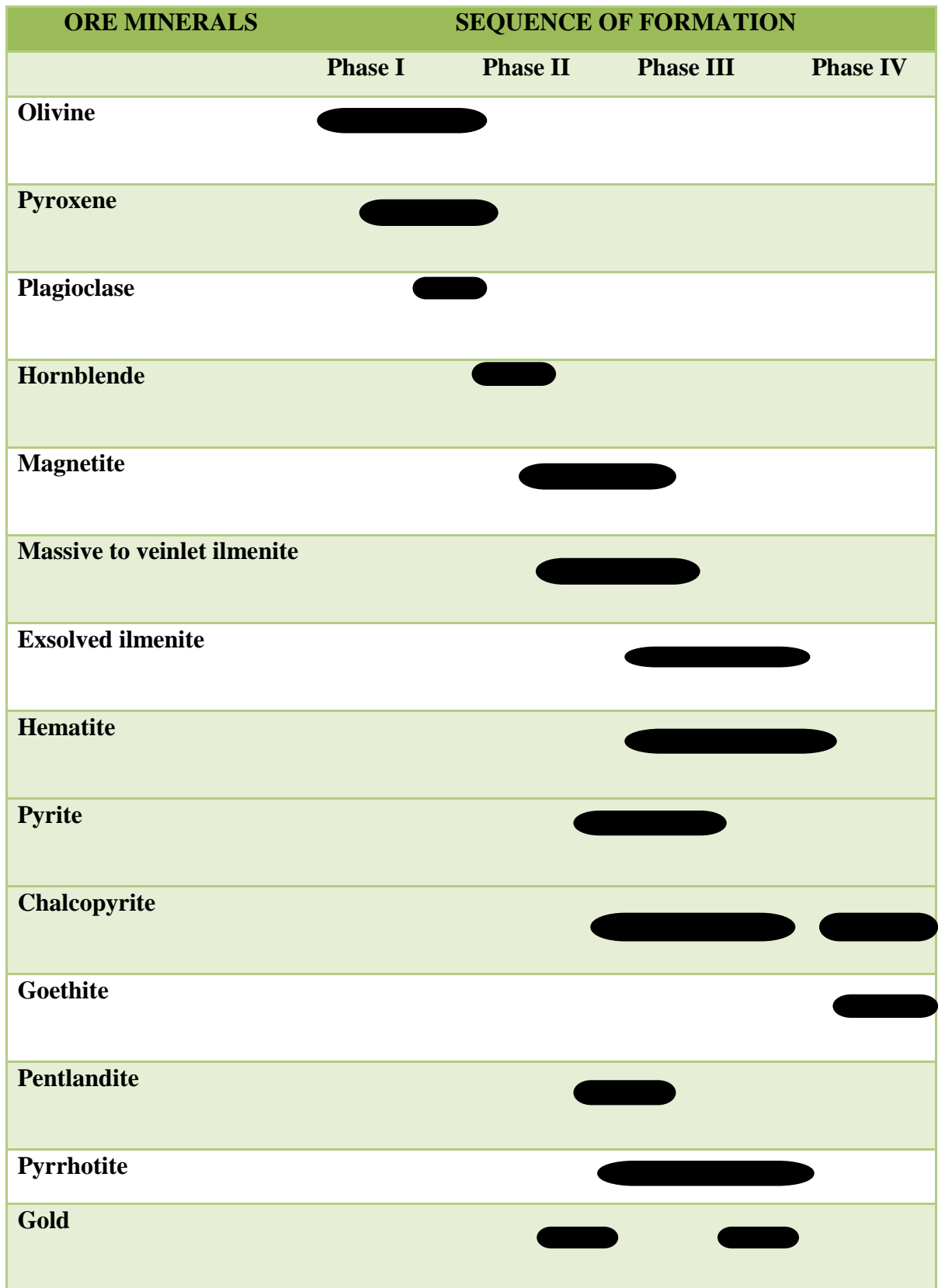


Figure.24. Mineral paragenetic sequences mineralization of Bikilal iron ore deposit.

Phase I

According to petrographic study the orders of major phase crystallization starts with olivine (big grain of size range from 2-6mm) (Fig.14 (A)), followed by pyroxene, plagioclase and later due to hydration of those anhydrous minerals hornblende minerals were crystalized. This idea is also supported by the geochemical results obtained by Woldemichael and Kimura (2008) (Fig.25).

Phase II

In the second phase of crystallization; poikilitic and veinlet (lath shaped) magnetite grains were crystalized later to the gangue silicate (Fig.21 (A, B, C & D)) – same as the poikilitic magnetite, massive- veinlet ilmenite following the gangue minerals were crystalized (Fig.22 (A)) – irregular grains of pentlandite (Fig.22 (A)) grows in association with pyrhotite. Poikilitic – veinlet (lath shaped) isolated grain of pyrite (Fig.22 (A & D)) co-precipitated together with chalcopyrite occurs as inclusion in the gangue minerals (Fig.22 (B & D)). Inclusion of free gold grains are also identified in gangue minerals.

Phase III

This phase is represented by mineral association of exsolved lamellar ilmenite in magnetite (Fig.20 (E)), hematite which is transformed from magnetite and ilmenite grains as an oxidation product (Fig.20 (B, D & E)), pyrhotite which occurs as inclusion in pentlandite is correspond to this phase (Fig.22 (A)) and chalcopyrite which is altered from pyrite and pyrhotite (Fig.21 (A)) were crystalized in this phase of mineralization. Gold grains occur as patched inclusion in chalcopyrite is also grouped in this phase (Fig.23 (B)).

Phase IV

Goethite which is the secondary hydration product of ilmenite, magnetite, hematite, chalcopyrite and pyrite is identifying in this phase of mineralization (Fig. 20 (A, C & E)) and (Fig.21 (A & B)). In addition to goethite, hydro- goethite is also identified in some sections due to intense hydration.

5.6. POSSIBLE HYPOTHESIS FOR BIKILAL IRON ORE GENESIS ACCORDING TO DIFFERENT AUTHORS

The formation of immiscible oxide melt from the silicate magma may have resulted from crystal fractionation, magma mixing, abrupt change in oxygen fugacity, and an introduction of fluids or P (Philpotts, 2008). Fe-Ti-rich oxide liquids may be the normal residue of mafic differentiation, concentrated in crystallize interstitially and late in anorthosite-hornblende gabbro (Philpotts, 2008). The Fe-rich melts separated from the ore bearing magma by liquid immiscibility were then injected along fractures and spaces between the gabbroic intrusions and wall-rocks (e.g., Veksler et al., 2008).

The ore-forming magma was emplaced near surface, the fluxing agents, mainly the phosphorus, facilitated development of immiscible oxide melt (Kolker, 1982, as cited in Zhou et al., 2005) during the liquid immiscibility. Moreover, the concentrations of other volatiles, e.g., F and Cl, could also have been elevated in the Fe-rich melts because their partition coefficients in apatite are higher than those in silicate melts (Webster et al., 2009). This Fe- and volatile-rich melt rose to the top of the magma chamber forcefully due to its low density (Hou et al., 2011).

The Bikilal gabbro magmas possibly formed by fractionation of mantle-derived magmas and enrichment of volatiles in the gabbroic magmas have been reached by fractionation of anhydrous minerals (e.g. olivine and clino-pyroxene).

Based on gabbroic textural analysis observed under microscope and by preexisting geochemical data the order of crystallization of major phases is olivine, followed by plagioclase and clinopyroxene. Woldemichael and Kimura (2008) suggest that crystallization of major silicate phases was followed by crystallization of magnetite –ilmenite, as these mostly occur in volume only in low MgO content samples. The olivine gabbros show linear geochemical trends (as shown by the MgO versus SiO₂, Al₂O₃, CaO, NaO, and K₂O contents), and the inflected trends for TiO₂ and FeO contents, suggestive of a crystallization sequence formed along with a fractionation of the source magma. The Fe - Ti oxide minerals

hosting these elements and phases are modally the most important in the MgO - poor samples (Fig.24).

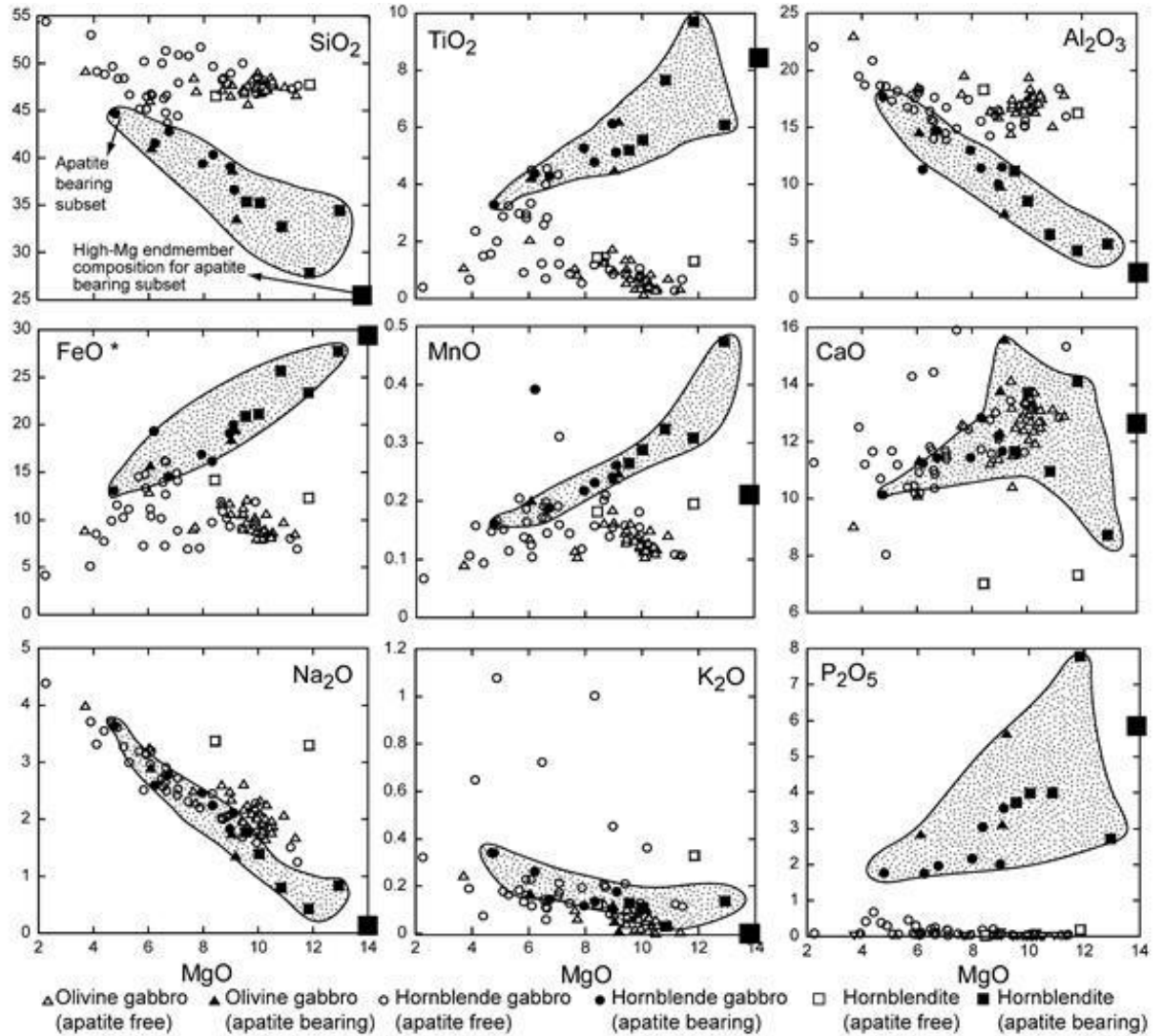


Figure.25. Major Element MgO variation diagrams for the Bikilal – Ghimbi gabbro. The end member was estimated using multiple least square regression calculations. Taken from Woldemichael and Kimura (2008)

Hornblende-bearing gabbroic rocks (xenoliths and plutons) are fairly common in subduction related magmatic suite and have been considered to represent magmatic differentiation process in arc magmas (Beard, 1986). The presence of hornblende as a dominant phase in gabbroic rocks of early crystallizing mineral from water bearing mafic magmas as a product of reaction of early crystallized cumulate (olivine, pyroxene and plagioclase) and water-rich evolved melt/aqueous fluid (Costa et al 2002). The hornblende gabbro and hornblendite in Bikilal represent altered equivalents of the olivine gabbro rather than being a separate intrusion from different parental magmas (Woldemichael and Kimura, 2008). Based on the interpretation of major element bulk rock chemistry the hornblende gabbros were produced by a metasomatism of the olivine gabbro (Woldemichael and Kimura, 2008).

Bikilal ilmenite – magnetite ore bodies are localized within the intrusive and their minerals are found as accessory in all the intrusive rocks either in disseminated or massive form; particularly they are localized with in hornblendite gabbro and in its vicinity.

The anorthosite- hornblende gabbro magma containing iron- titanium was separated in two phases due to time or space. First the magma was separated into olivine gabbro occupying the central part of the intrusive, and anorthosite- hornblende laying on the margin of the intrusive, next the anorthosite magma was differentiated to many of its varieties and massive ores. Finally the anorthosite rocks were enriched with titanium mineral.

Among the iron ores in the world, there is specific mineral assemblage, i.e. magnetite-hematite-apatite, called ‘Kiruna’-type iron deposits, which are characterized by sulphide-poor low-Ti magnetite-fluorapatite-actinolite assemblage, and ore types containing many hundreds of millions of tons of high-grade massive iron ore, to small vein and veinlet ores (Hildebrand 1986; Nystrom and Henriquez 1994, as cited in Hou et al., 2011). Kiruna type ore universally refer to high – phosphorus iron ores (Guilbert and Park, 1986). Bikilal magnetite –ilmenite deposit in the western wollega has various mineralogical and geochemical characteristics that are typical of the Kiruna type magnetite- ilmenite -apatite end member. Therefore, based on the similarity found Bikilal iron ore deposit is a Kiruna-type deposit.

6.1. CONCLUSION

Bikilal magnetite- ilmenite ore deposit is believed to be the segment of Pan-African Orogeny of the Mozambique Belt. The major lithological units are olivine gabbro, hornblende gabbro and hornblendites with minor pegmatite, granite, migmatite, and anorthosite intrusive rocks. The major structural trends in Bikilal are reflected in regional lineaments of the study area trending NW – SE. Faults in this area do not display pronounced displacement. Bikilal-gabbroic complex consists of olivine gabbro in the central part of the intrusions, hornblende gabbro and hornblendites at periphery.

The spatial association of the magnetite- ilmenite iron ore body with gabbroic intrusive igneous rocks clearly indicates genetic relationship between mafic magmatism and iron ore formation. Bikilal iron ore deposit has various mineralogical characteristics that are typical of Kiruna type magnetite- ilmenite end member. The microscopic studies, field relationships and the overall geological evidence at Bikilal indicate that the hornblendite gabbro, hornblende gabbro and anorthosite intrusive rocks are the host.

The paragenetic sequence of Bikilal iron ore deposit start with the magmatic differentiation through liquid immiscibility and crystallization of high temperature olivine followed by pyroxene later feldspars. The hornblende in Bikilal intrusive is the product of hydration of anhydrate olivine which is due to metasomatism effect. After the crystallization of the olivine and other silicate minerals out of the mafic melt the Fe-Ti oxide and sulphide containing liquid is left in melt and later start to crystalize with the introduction of phosphate due to super replenishment of the magma in shallow depth.

Hematite and goethite minerals are present near the surface condition and they are product of surface weathering of ilmenite and magnetite of hydration and oxidation. In some polished section specimen hematite show an exsolved plate in the ilmenite justifying the solidus transformation of magnetite to ilmenite and later to hematite. Goethite is further transformed

to hydro-goethite. The sulphides like pyrite occur adjacent to ilmenite and magnetite as disseminated inclusions in the silicate. Secondary pyrite grains are found as a replacement of the pyrrhotite mineral. Chalcopyrites are found as inclusion inside the gangue and as a replacement of early formed pyrrhotite. Gold occurs as inclusion in chalcopyrite grains and in some sections as minute free grains. According to the ore microscopic study pyrite crystals found as poikilitic inclusion in hornblende gabbro so that crystallized at the same time with magnetite and massive-veinlet ilmenite grains.

Finally the paragenetic sequence is identified into four stages as follows according their relative time of formation:

Phase I = Silicates (Olivine + Pyroxene+ Feldspar)

Phase II =Magnetite + Massive- Veinlet Ilmenite + Pyrite + Pentlandite+ Gold +Pyrite

Phase III =Exsolved Ilmenite + Hematite+ Pyrrhotite +Gold

Phase IV=Chalcopyrite + Goethite

In this work mineral association of Fe-Ti oxide- Py-Cu-Pyr-Ni-Au mineralization were identified and studied. Chloritization, sericitization, tremolitization, and oxidation alteration have been observed in hornblende gabbro found at the periphery of the intrusion.

6.2. RECOMMENDATIONS

1. Further investigation on the feasibility study, advanced techniques for beneficiation and to upgrade the quality of the Bikilal iron deposit should be done to assess the economic asset of the Fe.
2. Previous works were motivated particularly for iron and phosphate deposit in this study area; however this work found an indication of possible gold mineral occurrence. Therefore detail and systematic exploration work should be conduct for gold mineral prospection in addition to iron and phosphate deposits to assess the economic value of the Gold.
3. This research work results mainly based on the petrography (thin section and ore microscopy) study and by utilizing preexisting geochemical data, but to have a confined and well established paragenetic sequence study the thermo barometry, isotope, and well defined major and trace element analysis have to be conduct. Therefore feature intended researcher or organization on this particular area should conduct this analysis to come up with a coherent and certain paragenetic sequence.

REFERENCES

- Abdelsalam, G., Liegeois, J.P., and Stern, J. (2002). The Saharan Metacraton. *Journal of African Earth Sciences*. **34**: 119–136.
- Alemu, T. and Abebe, T. (2000). Geology of the Gimbi area. Unpublished technical report, Geological Survey of Ethiopia, Addis Ababa, Ethiopia.
- Asrat, A., Barbey, P. and Gleizes, G. (2001). The Precambrian Geology of Ethiopian. *African Geoscience review*, **8**(3): 271-288, France.
- Beshawered, E., (2001). Geology and Phosphate Mineralization of Ghimbi-Bikilal Area Western Wollega Zone, Oromia National Regional State. Unpublished technical report, Ministry of Mines Geological Survey of Ethiopia, Agrominerals Exploration Project, Addis Ababa, Ethiopia.
- Blasband, B., White, S., Brooijmans, P., Boorder, H. & Visser, W. (2000). Late Proterozoic extensional collapse in the Arabian–Nubian Shield. *Journal of the Geological Society of London*. **157** (2000): 615–628.
- Bowring, S.A., and Williams, I.S. (1999). Priscoan (4.00–4.03) orthogneisses from northwestern Canada: Contributions to Mineralogy and Petrology, **134**: 3–16.
- Brown, T.G., Bide, T., Hannis, S. D., Hetherington, L.E., Idoine, N.E., Shaw, R.A., Walters, A.S., Lusty, P.A.J. and Kendall, R., (2010). World mineral production 2004-08. Unpublished technical report, British Geological Survey.
- Buddington, A.F. and Lindsley, D.H. (1964). Iron-titanium oxide minerals and synthetic equivalents. *Journal of petrology*. **5**: 310 -357.
- Conliffe, J., Kerr, A. & Hanchar, D. (2012). Mineral Commodities of Newfoundland and Labrador iron ore. Geological Survey, Mineral Commodities Series, Number 7.
- Consult 4 International (1996). Interim Report No.1 & 2. Bikilal phosphate Project. Unpublished report, Geological Survey of Ethiopia, Addis Ababa, Ethiopia.
- Costa, F., Dunga, M.A. and Singer, B.S. (2002). Hornblende- and Phlogopite- bearing Xenoliths from volcan San Pedro (360S), Chilean Andes: Evidence for Melt and Fluid Migration and Reaction in Subduction- Related plutons. *Journal of petrology*. **43**:219-241.
- Eric C. Ferré, Stephanie M. Maes, Kevin C. and Butak (2009). The magnetic stratification of

- layered mafic intrusions; Natural examples and numerical models, *Lithos.* **111**: 83–94.
- Ethio-Korean Iron Exploration Project (1986, 1988). Ethio Korean Iron Exploration and deposit Evaluation in central and Western Wollega. Unpublished technical report, Ethiopia Geological Survey, Addis Ababa, Ethiopia.
- Ethiopian Central Metrological Agency, Ghimbi Station, 10 year average unpublished report, 2013
- Fortune newsletter, (2012). Published on July 29. WWW. Addisfortune.com, **13**: 639
- Gaudette, E. and Hurley, M. (1979). Where were the Pan African Mountains? No evidence of 500 M.Y. detrital zircons. *Tectonophysics* **54**: 211-230.
- Geological survey of Ethiopia (2010). Opportunities for iron resources development in Ethiopia. Unpublished technical report, geoscience data center, Addis Ababa, Ethiopia.
- Gebre, W., (2010). Geology and Mineralization of Bikilal Phosphate deposit, Western Ethiopia, Implication and outline of gabbro intrusion to East Africa Zone. *Iranian Journal of Earth Sciences.* **2**: 158-167.
- Guilbert, M. and Park, JR., (1986). The geology of ore deposits, W.H. Freeman and Company, New York.
- Hildebrand S. (1986). Kiruna-type deposits: their origin and relationship to intermediate subvolcanic plutons in the Great Bear Magmatic Zone, northwest Canada. *Econ. Geol.* **81**: 640–659.
- Hou, T., Zhang, T. and Kusky, T. (2011). Gushan magnetite–apatite deposit in the Ningwu basin, Lower Yangtze River Valley, SE China: Hydrothermal or Kiruna-type? *Ore Geology Reviews.* **43**: 333–346.
- Jayanthu, S., Sa, B.K, Pitoshe, S., and Alok, R.S. (2010). Overview of Iron ore mining in India Vis-A-Vis status of Production in 2020 AD. Unpublished technical report, National Institute of technology, ORISSA, India.
- Kazmin, V., Shifferaw, A. and Balch, T. (1978). The Ethiopian Basement: Stratigraphy and Possible Manner of Evolution. *Geologische Rundschau.* **67**: 531—546.
- Kazmin, V., (1973). Geology of Ethiopia. Unpublished Technical report, Ministry of mines geological survey of Ethiopia, Addis Ababa, Ethiopia.
- Kebede, T., Kloetzli, U. S. and Koeberl, C. (2001). U/Pb and Pb/Pb zircon ages from

- granitoid rocks of Wallagga area: constraints on magmatic and tectonic evolution of Precambrian rocks of western Ethiopia. *Mineralogy and Petrology*, Austria. **71**: 251-271.
- Kennedy Q. (1964). The structural differentiation of Africa in the Pan-African (500 m.y.) tectonic episode. Univ. of Leeds, 8th Ann. Rep., p. 48-49
- Kirk, S. (2000). Iron ore. U.S. Geological Survey Minerals Yearbook.
- Kröner, A. (1980). Pan African Crustal Evolution. In: Proceeding at the 5th Conference on African Geology Vol. 1980, No. 2. , Cairo, Egypt.
- Kröner, A. and Stern, J. (2004). Pan-African Orogeny North African Phanerozoic Rift Valley. *Encyclopedia of Geology*.
- Meert, J., (2002). A synopsis of events related to the assembly of eastern Gondwana. *Tectonophysics*.**6800**:1 – 40.
- Nyström, J., Henriquez, F. (1994). Magmatic features of iron ores of the Kiruna type in Chile and Sweden: ore textures and magnetite geochemistry. *Econ. Geol.* **89**: 820–839.
- Philpotts', R. (2008). Comments on: Liquid Immiscibility and the Evolution of Basaltic Magma. *Journal of petrology*. **49**: 2171 – 2175.
- Scott W., Jackson A. and Dunham C. (2000). Ore mineral associations and industrial minerals in the ultramafic rocks of Jamaica and Tobago. *Caribbean Journal of Earth Science*. **34**: 5-16.
- Stern J, Avigad D, Miller R and Beyth M. (2006). Evidence for the Snowball Earth hypothesis in the Arabian-Nubian Shield and the East African Orogen. *Journal of African Earth Sciences*. **44**:1–20.
- Stern, J. (1994). Arc assembly and Continental Collision in The Neoproterozoic East African Orogen: Implications for the Consolidation of Gondwanaland. *Annu. Rev. Earth Planet. Sci*: **22**: 319-51.
- Stern, J. and Scholl, W. (2010). Yin and yang of continental crust creation and destruction by plate tectonic processes. *International Geology Review*. 52:1–31.
- Tadesse, S. (2009). Mineral Resources Potential of Ethiopia , Addis Ababa University printing press, Addis Ababa, Ethiopia.
- U.S. Geological Survey (2011). Mineral commodity summaries.
- USGS (2011). Mineral commodity summery 2011.

- USGS, (2013). Mineral commodity summaries, U.S. Geological Survey, Reston, Virginia, 198 p.
- Veksler, V., Dorfman, M., Borrisov, A., Wirth, R. and Dingwell, B. (2008). Liquid Immiscibility and Evolution of Basaltic Magma: Reply to S.A. Morse, A.R. Mc Birney and A. R. Philpotts. *Journal of Petrology*. **49**: 2177-2186
- Webster, J.D., Tappen, C.M., Mandeville, C.W. (2009). Partitioning behavior of chlorine and fluorine in the system apatite–melt–fluid. II: Felsic silicate systems at 200 MPa. *Geochim. Cosmochim.* **73**: 559–581.
- Western Wollega, Ghimbi Zone Agriculture and Urban Development Bureau, unpublished report, 2012
- Woldemichael, B. and Kimura, J. (2008). Petrogenesis of the Neoproterozoic Bikilal-Ghimbi gabbro, Western Ethiopia. *Journal of Mineralogical and Petrological Sciences*. **103**: 23– 46.
- Woldemichael, B., Kimura, J, Dunkley, J., Tani, K., & Ohira, H. (2010). SHRIMP U–Pb zircon geochronology and Sr–Nd isotopic systematics of the Neoproterozoic Ghimbi-Nedjo mafic to intermediate intrusions of Western Ethiopia: a record of passive margin magmatism at 855 Ma. *International Journals of Earth Science*. **99**: 1773–1790.
- Wood, B., (2011). The formation and differentiation, Oxford University, physics today. UK.
- Zhou, F., Robinson, T., Leshner, C., Keays, R., Zhang, C. and Malpas, J. (2005). Geochemistry, Petrogenesis and Metallogenesis of the Panzhihua Gabbroic Layered Intrusion and Associated Fe–Ti–V Oxide Deposits, Sichuan Province, SW China. *Journal of Petrology*. **46**: 2253–2280.

APPENDIX I

Table: Drillhole location

S.No.	Station- No	Easting	Northing	Elevation	Angle and dip of hole	Depth
1	Bk-502	816838.99	1031120.02	1972.20	Vertical	200.95
2	BK-503	816839.47	1031069.91	1967.20	Vertical	261.15
3	BK-504	816887.80	1031069.61	1976.18	Vertical	202.0
4	BK-510	817137.09	1030721.48	1969.48	Vertical	205.4
5	BK-514	816690.28	1031273.01	1968.87	Vertical	246.29
6	BK-515	816640.18	1031324.35	1979.22	Vertical	231.18
7	BK-516	816542.35	1031329.34	1956.28	Vertical	210.27
8	BK-520	816639.05	1031274.13	1955.79	Vertical	249.38
9	BK-522	816441.53	1031284.50	1919.60	Vertical	249.28
10	BK-601	816582.67	1032111.25	1743.61	60 ⁰ north	250.16
11	BK-602	816783.93	1032035.07	1793.09	60 ⁰ north	348.68
12	BK-604	816994.19	1032082.80	1795.07	60 ⁰ north	298
13	BK-605	817095.53	1032103.53	1738.41	60 ⁰ north	311.53
14	BK-606	817178.89	1032164.04	1724.00	60 ⁰ north	350.86
15	BK-607	817254.00	1031957.00	1732.60		15
16	BK-608	817440.19	1031862.40	1729.30	60 ⁰ NE	264.73
17	BK-609	817600.99	1031740.19	1732.20	N45E	350.93
18	BK-610	816178.15	1032051.09	1702.46	60 ⁰ north	300.03
19	BK-611	816416.16	1032143.53	1712.50	60 ⁰ north	254.98
20	BK-612	817573.00	1031878.23	1732.13	60 ⁰ N45E	207.5
21	BK-613	817364.86	1031594.47	1798.38	60 ⁰ N45E	261.08
22	BK-614	817701.00	1031557.00	1755.67	60 ⁰ N45E	208
23	BK-615	817804.00	1031372.00	1771.90	60 ⁰ N45E	159.13
24	BK-616	817857.00	1031148.00	1826.26	60 ⁰ N45E	130.2

APPENDIX II

Table.2. Iron ore occurrence and deposits of Ethiopia; taken from (Solomon Tadesse, 2009).

Location	Status	Lon g.	Lat.	Estimated Reserve	Ore Type	Geology
Adua (Tigray)	Mineral occurrence	38.9 6	14.1 4	5Mt(Adua+ Axum+ Enticho)	Magnetite Limonite	Gossan Related Deposit Au,Ag,Zn
Aira (Wollega)	Mineral occurrence	35.3 6	9.06	<10 Mt	Hematite Magnetite	Weathered Basalt
Assale (Tigray)	Mineral Occurrences	40.0 6	14.3 8	<10 Mt	Magnetite	Unspecified ore Deposit Type
Beligal (Tigray)	Mineral occurrences	39.9 9	14.3 9	No data	Magnetite limonite	Unspecified ore deposit type
Bikilal (Wollega)	Industrial project	35.8 0	9.37	57 Mt	Magnetite	Ore deposit hosted by basic intrusions: Fe, Ti, V, Ni-Cu, (Au,Co)
Billa (Wollega)	Mineral occurrence	35.5 9	9.34	No data	Hematite Magnetite – Hematite	Gossan related deposit: Au, Ag, Zn
Bissidimo (Harar)	Mineral occurrence	42.1 9	9.19	No data	Hematite Limonite	Cretaceous sediment
Chago (Wollega)	Mineral Occurrences	35.6 0	9.17	0.20 Mt. 64% Fe	Magnetite– Hematite,	Gossan (VMS, MVT, Veins, etc.

	ce					Limonite-Hematite	related deposits: Au, Ag, Zn)
Chilachik m (Tigray)	Mineral occurrences	38.41	13.87	No data		Hematite	Gossan (VMS, MVT, Veins, etc. related deposits: Au, Ag, Zn)
Dimma (Wollega)	Mineral occurrence	35.58	8.95	0.05 Mt, 65% Fe		Hematite, Magnetite, Limonite-Hematite, Magnetite-Hematite	Gossan (VMS, MVT, veins, Au, Ag, Zn)
Enticho (Tigray)	Mineral occurrences	39.12	14.23	See above		Limonite	Gossan related deposits: Au, Ag, Zn
Famasari (Wollega)	Mineral occurrences			65-68% Fe		Hematite-Magnetite	Gossan: related deposits: Au, Ag, Zn, Ni, Pt
Gelatti (Wollega)	Mineral occurrences	41.14	9.01	No data		Hematite, Magnetite, Martite	Unspecified ore deposit type
Gambo (Wollega)	Mineral Occurrences	35.51	9.50	No data		Magnetite	Gossan (VMS, MVT, veins, Au, Ag, Zn)

Locality	Status	Lon g.	Lat .	Estimate d Reserve	Ore Type	Geology
Gamalucho (Kaffa)	Deposit or prospect	37.2 1	7.5 9	12.50Mt	Magnetite	Laterite – Related ore Fe,Mn, Ni-Co, Au, Pt, Corundum, P,REE,Nb
Garro (Kaffa)	Mineral occurrenc es	37.1 9	7.5 1	12.50 Mt	Hematite Limonite	Related ore deposits:Fe, Mn, Ni- Co, Au, Pt,orundum,P,REE,N b
Gato (Mai Guda)(Kaffa)	Mineral occurrenc e	37.1 7	7.4 1	0.075 Mt, 40% Fe	Hematite Limonite	Laterite- related ore deposits: F, Mn, Ni- Co, Au, Pt, Corundum, P, Ree, Nb
Ghimira basin (Kaffa)	Mineral occurrence s	36.0 1	7.0 2	No data	Hematite Limonite	Gossan related ore type
Gordona (Korree) (Wollega)	Deposit	35.5 4	8.7 7	0.27 Mt, 63% Fe	Magnetite -Hematite Magnetite	Gossan related ore type
Kata Valley (Wollega)	Mineral occurrenc e	35.6 2	9.4 9	0.40 Mt, 69% Fe	Magnetite Martite	Gossan: (VMS, MVT, related deposits: Au)
Kenticha (Sidamo)	Mineral occurrenc e	39.1 8	5.1 9	No data	Magnetite	Ore deposits related to basic ultrabasic magmatic rocks
Kunni (Harar)	Mineral occurrenc	40.9 4	8.9 4	No data	Hematite Magnetite	Unspecified ore type

	e					
Kurkure (kaffa)	Mineral occurrence	37.28	7.38	No data	Hematite Limonite	Gossan related ore type
Like (kaffa)	Mineral occurrence	37.29	7.49	No data	Hematite Limonite	Gossan related ore types
Melka Arba (Sidamo)	Prospect	39.55	6.32	4.60 Mt		Related to basic intrusion
Melka Sedi (Kaffa)	Deposit or prospect	37.39	7.50	12.50Mt	Hematite limonite	Laterite –Related ore Fe,Mn,Ni-Co, Au, Corundum, P, REE, Nb, Pt
Shakisso (Sidamo)	Mineral occurrence	38.63	5.22	No data	Magnetite	Ore deposits related to basic ultrabasic magmatic rocks
Soka (harar)	Mineral occurrence	41.48	9.14	No data	Hematite	Unspecified ore type
Tulu Bollale (Wollega)	Mineral occurrence	35.71	9.49	No data	Hematite - Magnetite Magnetite - Hematite	Gossan (VMS, MVT, Au, Ag, Zn)

Locality	Status	Long.	Lat.	Estimated Reserve	Ore Type	Geology
Ujau (Harar)	Mineral occurrence	41.42	9.25	No data	Hematite-Magnetite	Unspecified ore
Wollega	Deposit or prospect	35.31	8.71	4.48 Mt	Magnetite-Hematite	Banded iron formations (BIF “Superior Fe”)
Worakalu (Wollega)	Mineral Occurrence	35.53	9.07	0.05 Mt, 62% Fe	Magnetite-Hematite	Gossan: (VMS, MVT, Veins, etc related deposits: Au,Ag,Zn)
Yubdo (Wollega)		35.49	8.93	0.05 Mt, 71% Fe	Magnetite	Laterite- related ore deposits: Fe,Mn,Ni-Co,Au, Corundum, P, REE, Nb,Pt
Abdi Berbere (Tigray)	Mineral occurrence	38.55	14.36	No data	Magnetite	Gossan(Vms, MVT, Veins, etc related deposits: Au,Ag,Zn)
Gambela-Dembidollo (Wollega)	Prospect or deposit	34.80	8.53	No data	Magnetite	Ore deposits in layered ring complexes (ural and Alaskan sub-type): PGE,Cr
Gimbi-Daleti (Wollega)	Prospect or deposit	35.05	8.85	No data	Magnetite	Anorthosite- Hosted ilmennite and ilmenite and

						hematite- ilmenite deposits:ti,Fe,V,(Cr, Mn,Ni)
Dombowa (Kaffa)	Prospect			12.50 Mt	Limonite	Laterite related ore deposit
Wankey (Area) Wabera–Kiltu (Wollega)	Prospect under (Upstream reconnaissance)	35.27	9.84	No data		Volcano-Sedimentary and sedimentary-exhalative ore deposits
Belowtuist (Wollega)	Mineral occurrence			2.50 Mt	Magnetite, Hematite, Limonite	Ferreginous quartzites,Au,REE, Pb,Ni,Pt